forming growth factor-β and fibronectin) and proinflammatory/proapoptotic genes (pancreatitis-associated protein, lysyl oxidase, sialoprotein, prostaglandin F2α receptor, galectin-5, enolase 1) were included among the 54 genes that were increased in HS rats but decreased in AMLO and TEMP rat. Several Ca-handling protein genes, such as voltage-dependent protein, T type protein, α1G subunit protein, S100 Ca-binding protein A4, cerebellar Ca-binding protein, and spot 35 protein genes were also included. By contrast, several genes, *i.e.*, aquaporin 9, CD74, vitronectin, mitogen-activated protein kinase kinase (MAPKK) and A-raf, were upregulated by the treatment with either amlodipine or Tempol.

Discussion

In the present study, we demonstrated the beneficial effects of the long-term CCB amlodipine on hypertensive heart failure. Treatment with amlodipine significantly reduced the heart weight, LV wall thickness and LV diameter, and improved LV systolic function. Increases in expression levels of the BNP and IL-1β gene were inhibited by the treatment with amlodipine. Moreover, we investigated the changes in the expression levels of a large number of genes in the hearts of LS, HS, AMLO and TEMP rats at the heart failure stage.

In this study, we used Tempol as an antioxidative drug. Tempol is a low–molecular-weight super oxide dismutase mimetic that is both metal-independent and cell membrane permeable. Several investigators have suggested that Tempol reduces O_2-induced damage during inflammation, radiation, and ischemic/reperfusion injury. Although Tempol improved the cardiac function and hypertrophy in our study, the mortality and the BW loss were not improved. This chemical compound may cause some systemic adverse effects. Since the inhibitory effect of Tempol on the hypertrophied heart is controversial, the mechanisms of the induction of the hypertrophy such as hypoxia (*34*), isoproterenol (*35*) or aldosterone (*36*) may be related to the difference.

Many factors, such as the renin-angiotensin system (*37*), calcineurin (*26*, *38*), the endothelin-system (*33*, *39*), and IL-1β (*33*), have been reported to be involved in the transition from compensated cardiac hypertrophy to decompensated heart failure in DS rats. They also include abnormalities in calcium handling, apoptosis of cardiac myocytes, increases in cytokine expression and extracellular matrix, and activation of neurohumoral factors. The DS rat develops systemic hypertension, depending on the amount of sodium supplied in the diet, and cardiac hypertrophy with interstitial fibrosis. Prolonged hypertension induces reduced myocardial contraction and relaxation velocities (*19*, *20*), indicating that this model fully recapitulates the phenotype of human LV hypertrophy and hypertensive heart failure.

Treatment with short-acting CCBs may worsen heart failure and increase the risk of death in patients with advanced LV dysfunction. Amlodipine can regulate membrane fluidity and cholesterol deposition, stimulate NO production to recruit its biologic actions, and regulate matrix deposition. Recognition of the ancillary actions of amlodipine is important for understanding the agent's mechanisms of action and the pathologic mechanisms underlying cardiovascular disease. The antioxidant properties of amlodipine are attributed to its chemical structure and direct physicochemical interactions with the membrane lipid bilayer, as evidenced by changes in membrane thermodynamic properties (*40*). Oxidative stress is widely known to play important roles in the pathophysiology of hypertensive heart failure. In the present study, treatment with amlodipine improved the degree of cardiac hypertrophy, dilatation, contraction and mortality. The improvement of cardiac fibrosis and a decrease in apoptosis may be involved in the mechanism of the beneficial effects of amlodipine. Although it is difficult to analyze the pathophysiological mechanism by which amlodipine inhibits the progression of heart failure, our finding that the drug altered the expression levels of various genes may provide a clue.

An antioxidative mechanism may be involved in the beneficial effects of amlodipine in heart failure. Amlodipine has been reported to inhibit oxidative stress in the hypertensive hypertrophied heart (*41*). By the treatment with amlodipine, 195 genes were changed and these genes may be involved in the beneficial effects of amlodipine on heart failure. Among these 195 genes, 110 genes were increased in HS rats and decreased in AMLO rats. In 110 genes, 54 genes were also decreased in TEMP rats. These genes that were changed in a similar fashion in AMLO and TEMP rats may be involved in the antioxidative mechanisms of amlodipine on hypertensive heart failure. Many of these genes have been classified as cell signaling–related genes. Since fibrosis-related genes such as arachidonate 12-lipoxygenase (*42*), transforming growth factor-β and fibronectin are known to be involved in the pathophysiology of cardiac fibrosis, they were changed similarly by the treatment with either amlodipine or Tempol. Proinflammatory and/or proapoptotic genes such as pancreatitis-associated protein, lysyl oxidase, sialoprotein, prostaglandin F2α receptor, galectin-5 and enolase 1 are also included in this group. Pancreatitis-associated protein is reported to be related to play a role in inflammatory pancreatitis (*43*). Lysyl oxidase is an enzyme involved in extracellular matrix maturation (*44*). Prostaglandin F2α is reported to have the ability to oxidize arachidonate. Galectin is a β-galactoside–binding protein that is related to the initiation of apoptosis. Enolase 1 is reported to be involved in the aging of neural cells (*45*). The role of these proteins in the failing heart is unknown, and further investigations will be needed. Since Ca-handling proteins have not previously been reported to be involved in the mechanism of CCB on the heart, several Ca-handling protein genes, such as the voltage-dependent, T type, α1G subunit, S100 Ca-binding protein A4, cerebellar Ca-binding protein, and spot 35 protein genes, are also included in this group. Further study is needed to clarify the effect of these genes.

In contrary, in 195 genes, 85 genes were decreased in HS rats and increased in AMLO rats. In 85 genes, 38 genes were

also increased in TEMP rats. These genes may be involved in the protective effects on heart failure. Some of these genes such as aquaporin 9, which is mostly changed, were not known as cardiovascular-related genes. Since macrophage migration inhibitory factor (MIF) is reported to delay the progression of apoptosis (*46*), CD74, which is known as an MIF-binding protein (*47*), may have important roles in the protective mechanism of amlodipine. Since the activation of coagulation is involved in the pathophysiology of heart failure, vitronectin, which is a co-factor along with plasminogen activator inhibitor 1 (*48*) for the inhibition of thrombin, is upregulated. Other changed genes may also have important roles in the beneficial mechanisms of amlodipine on the heart. A novel mechanism of amlodipine on the development of heart failure may become obvious by use of our result.

In conclusion, the present study demonstrated that the long-term CCB amlodipine has beneficial effects on a hypertensive heart failure model. A genome-wide study using a gene chip provided various clues that should be useful for determining the beneficial antioxidative mechanisms of amlodipine on hypertensive heart failure.

Acknowledgements

We thank Reiko Kobayashi, Emi Fujita, Megumi Ikeda, Akane Furuyama, and Yuko Ohtsuki for their technical assistance.

References

1. Levy D, Garrison RJ, Savage DD, *et al*: Prognostic implications of echocardiographically determined left ventricular mass in the Framingham Heart Study. *N Engl J Med* 1990; **322**: 1561–1566.
2. Frohlich ED: Cardiac hypertrophy in hypertension. *N Engl J Med* 1987; **317**: 831–833.
3. Katz AM: The cardiomyopathy of overload: an unnatural growth response in the hypertrophied heart. *Ann Intern Med* 1994; **121**: 363–371.
4. Tavi P, Laine M, Weckstrom M, *et al*: Cardiac mechanotransduction: from sensing to disease and treatment. *Trends Pharmacol Sci* 2001; **22**: 254–260.
5. Komuro I: Molecular mechanism of cardiac hypertrophy and development. *Jpn Circ J* 2001; **65**: 353–358.
6. Chobanian AV, Bakris GL, Black HR, *et al*, National Heart, Lung, and Blood Institute Joint National Committee on Prevention, Detection, Evaluation, and Treatment of High Blood Pressure; National High Blood Pressure Education Program Coordinating Committee: The Seventh Report of the Joint National Committee on Prevention, Detection, Evaluation, and Treatment of High Blood Pressure: the JNC 7 report. *JAMA* 2003; **289**: 2560–2572.
7. Wilcox RG, Hampton JR, Banks DC, *et al*: Trial of early nifedipine in acute myocardial infarction: the Trent study. *Br Med J* 1986; **293**: 1204–1208.
8. The Israeli Sprint Study Group: Secondary prevention reinfarction Israeli nifedipine trial (SPRINT). A randomized intervention trial of nifedipine in patients with acute myocardial infarction. *Eur Heart J* 1988; **9**: 354–364.
9. Furberg CD, Psaty BM, Meyer JV: Nifedipine. Dose-related increase in mortality in patients with coronary heart disease. *Circulation* 1995; **92**: 1326–1331.
10. Spinale FG, Mukherjee R, Krombach RS, *et al*: Chronic amlodipine treatment during the development of heart failure. *Circulation* 1998; **98**: 1666–1674.
11. Lubsen J, Wagener G, Kirwan BA, *et al*: Effect of long-acting nifedipine on mortality and cardiovascular morbidity in patients with symptomatic stable angina and hypertension: the ACTION trial. *J Hypertens* 2005; **23**: 641–648.
12. Poole-Wilson PA, Lubsen J, Kirwan BA, *et al*: Effect of long-acting nifedipine on mortality and cardiovascular morbidity in patients with stable angina requiring treatment (ACTION trial): randomised controlled trial. *Lancet* 2004; **364**: 849–857.
13. Mason RP, Campbell SF, Wang SD, Herbette LG: Comparison of location and binding for the positively charged 1,4-dihydropyridine calcium channel antagonist amlodipine with uncharged drugs of this class in cardiac membranes. *Mol Pharmacol* 1989; **36**: 634–640.
14. Zhang X, Hintze TH: Amlodipine releases nitric oxide from canine coronary microvessels: an unexpected mechanism of action of a calcium channel–blocking agent. *Circulation* 1998; **97**: 576–580.
15. Cominacini L, Pasini AF, Pastorino AM, *et al*: Comparative effects of different dihydropyridines on the expression of adhesion molecules induced by TNF-alpha on endothelial cells. *J Hypertens* 1999; **17**: 1837–1841.
16. Ikeda U, Hojo Y, Ueno S, Arakawa H, Shimada K: Amlodipine inhibits expression of matrix metalloproteinase-1 and its inhibitor in human vascular endothelial cells. *J Cardiovasc Pharmacol* 2000; **35**: 887–890.
17. Mason RP, Marche P, Hintze TH: Novel vascular biology of third-generation L-type calcium channel antagonists: ancillary actions of amlodipine. *Arterioscler Thromb Vasc Biol* 2003; **23**: 2155–2163.
18. Rapp JP, Wang SM, Dene H: A genetic polymorphism in the renin gene of Dahl rats cosegregates with blood pressure. *Science* 1989; **243**: 542–544.
19. Inoko M, Kihara Y, Morii I, *et al*: Transition from compensatory hypertrophy to dilated, failing left ventricles in Dahl salt-sensitive rats. *Am J Physiol* 1994; **267**: H2471–H2482.
20. Inoko M, Kihara Y, Sasayama S: Neurohumoral factors during transition from left ventricular hypertrophy to failure in Dahl salt-sensitive rats. *Biochem Biophys Res Commun* 1995; **206**: 814–820.
21. Iwanaga Y, Kihara Y, Hasegawa K, *et al*: Cardiac endothelin-1 plays a critical role in the functional deterioration of left ventricles during the transition from compensatory hypertrophy to congestive heart failure in salt-sensitive hypertensive rats. *Circulation* 1998; **98**: 2065–2073.
22. Nishikawa N, Masuyama T, Yamamoto K, *et al*: Long-term administration of amlodipine prevents decompensation to diastolic heart failure in hypertensive rats. *J Am Coll Cardiol* 2001; **38**: 1539–1545.
23. Duggan DJ, Bittner M, Chen Y, Meltzer P, Trent JM: Expression profiling using cDNA microarrays. *Nat Genet* 1999; **21**: 10–14.
24. Shiffman D, Porter JG: Gene expression profiling of cardio-

vascular disease models. *Curr Opin Biotechnol* 2000; **11**: 598–601.
25. Hasegawa H, Yamamoto R, Takano H, *et al*: 3-Hydroxy-3-methylglutaryl coenzyme A reductase inhibitors prevent the development of cardiac hypertrophy and heart failure in rats. *J Mol Cell Cardiol* 2003; **35**: 953–960.
26. Shimoyama M, Hayashi D, Zou Y, *et al*: Calcineurin inhibitor attenuates the development and induces the regression of cardiac hypertrophy in rats with salt-sensitive hypertension. *Circulation* 2000; **102**: 1996–2004.
27. Liu YH, Carretero OA, Cingolani OH, *et al*: Role of inducible nitric oxide synthase in cardiac function and remodeling in mice with heart failure due to myocardial infarction. *Am J Physiol Heart Circ Physiol* 2005; **289**: H2616–H2623.
28. Ishii M, Hashimoto S, Tsutsumi S, *et al*: Direct comparison of GeneChip and SAGE on the quantitative accuracy in transcript profiling analysis. *Genomics* 2000; **68**: 136–143.
29. Lockhart DJ, Dong H, Byrne MC, *et al*: Expression monitoring by hybridization to high-density oligonucleotide arrays. *Nat Biotechnol* 1996; **14**: 1675–1680.
30. Lee CK, Klopp RG, Weindruch R, *et al*: Gene expression profile of aging and its retardation by caloric restriction. *Science* 1999; **285**: 1390–1393.
31. Mizukami M, Hasegawa H, Kohro T, *et al*: Gene expression profile revealed different effects of angiotensin II receptor blockade and angiotensin-converting enzyme inhibitor on heart failure. *J Cardiovasc Pharmacol* 2003; **42**: S1–S6.
32. Ikeda S, Hamada M, Qu P, *et al*: Relationship between cardiomyocyte cell death and cardiac function during hypertensive cardiac remodelling in Dahl rats. *Clin Sci* 2002; **102**: 329–335.
33. Shioi T, Matsumori A, Kihara Y, *et al*: Increased expression of interleukin-1 beta and monocyte chemotactic and activating factor/monocyte chemoattractant protein-1 in the hypertrophied and failing heart with pressure overload. *Circ Res* 1997; **81**: 664–671.
34. Elmedal B, de Dam MY, Mulvany MJ, *et al*: The superoxide dismutase mimetic, tempol, blunts right ventricular hypertrophy in chronic hypoxic rats. *Br J Pharmacol* 2004; **141**: 105–113.
35. Zhang GX, Kimura S, Nishiyama A, *et al*: Cardiac oxidative stress in acute and chronic isoproterenol-infused rats. *Cardiovasc Res* 2005; **65**: 230–238.
36. Yoshida K, Kim-Mitsuyama S, Wake R, *et al*: Excess aldosterone under normal salt diet induces cardiac hypertrophy and infiltration *via* oxidative stress. *Hypertens Res* 2005; **28**: 447–455.
37. Yamamoto K, Masuyama T, Sakata Y, *et al*: Roles of renin-angiotensin and endothelin systems in development of diastolic heart failure in hypertensive hearts. *Cardiovasc Res* 2000; **47**: 274–283.
38. Hayashida W, Kihara Y, Yasaka A, Sasayama S: Cardiac calcineurin during transition from hypertrophy to heart failure in rats. *Biochem Biophys Res Commun* 2000; **273**: 347–351.
39. Iwanaga Y, Kihara Y, Inagaki K, *et al*: Differential effects of angiotensin II *versus* endothelin-1 inhibitions in hypertrophic left ventricular myocardium during transition to heart failure. *Circulation* 2001; **104**: 606–612.
40. Mason RP, Walter MF, Trumbore MW, Olmstead EG Jr, Mason PE: Membrane antioxidant effects of the charged dihydropyridine calcium antagonist amlodipine. *J Mol Cell Cardiol* 1999; **31**: 275–281.
41. Umemoto S, Tanaka M, Kawahara S, *et al*: Calcium antagonist reduces oxidative stress by upregulating Cu/Zn superoxide dismutase in stroke-prone spontaneously hypertensive rats. *Hypertens Res* 2004; **27**: 877–885.
42. Wen Y, Gu J, Peng X, Zhang G, Nadler J: Overexpression of 12-lipoxygenase and cardiac fibroblast hypertrophy. *Trends Cardiovasc Med* 2003; **13**: 129–136.
43. Niederau C, Schonberg M: New developments in the pathophysiology of inflammatory pancreatic disease. *Hepatogastroenterology* 1999; **46**: 2722.
44. Raposo B, Rodriguez C, Martinez-Gonzalez J, Badimon L: High levels of homocysteine inhibit lysyl oxidase (LOX) and downregulate LOX expression in vascular endothelial cells. *Atherosclerosis* 2004; **177**: 1–8.
45. Poon HF, Vaishnav RA, Butterfield DA, *et al*: Proteomic identification of differentially expressed proteins in the aging murine olfactory system and transcriptional analysis of the associated genes. *J Neurochem* 2005; **94**: 380–392.
46. Baumann R, Casaulta C, Simon D, Conus S, Yousefi S, Simon HU: Macrophage migration inhibitory factor delays apoptosis in neutrophils by inhibiting the mitochondria-dependent death pathway. *FASEB J* 2003; **17**: 2221–2230.
47. Leng L, Metz CN, Fang Y, *et al*: MIF signal transduction initiated by binding to CD74. *J Exp Med* 2003; **197**: 1467–1476.
48. Xiang G, Schuster MD, Seki T, *et al*: Down-regulation of plasminogen activator inhibitor 1 expression promotes myocardial neovascularization by bone marrow progenitors. *J Exp Med* 2004; **200**: 1657–1666.

STEM CELLS
TISSUE-SPECIFIC STEM CELLS

A Comparison of Neural Differentiation and Retinal Transplantation with Bone Marrow-Derived Cells and Retinal Progenitor Cells

MINORU TOMITA,[a] TAISUKE MORI,[b,c] KAZUICHI MARUYAMA,[a] TASNEEM ZAHIR,[a] MATTHEW WARD,[a] AKIHIRO UMEZAWA,[b] MICHAEL J. YOUNG[a]

[a]The Schepens Eye Research Institute, Department of Ophthalmology, Harvard Medical School, Boston, Massachusetts, USA; [b]Department of Reproductive Biology and Pathology, National Research Institute for Child Health and Development, Tokyo, Japan; [c]Department of Pathology, Keio University, Tokyo, Japan

Key Words. Bone marrow stromal cells • Microglia • Retinal stem cells • Retinal transplantation • Neural differentiation

ABSTRACT

Retinal progenitor cells (RPCs) are immature precursors that can differentiate into retinal neurons, including photoreceptors. Recently, it has been reported that bone marrow-derived cells may also be capable of differentiation into cells of central nervous system lineage, including retinal neurons. We compared these two cell types to evaluate their potential as a source of cells for retinal transplantation. Marrow stromal cells (MSCs) and macrophages were isolated from enhanced green fluorescence protein mice. MSCs were cultured with brain-derived neurotrophic factor, nerve growth factor, and basic fibroblast growth factor to induce neuronal differentiation. RPCs were cultured under the same conditions or with 10% fetal bovine serum. Neuronal marker expression was examined and compared between MSCs and RPCs. MSCs, macrophages, and RPCs were also cultured with explanted retinas from rhodopsin knockout mice to study their potential for retinal integration. MSCs expressed neuronal and retina-specific markers by reverse transcription-polymerase chain reaction and immunocytochemistry. Both types of cells migrated into retinal explants and expressed neurofilament 200, glial fibrillary acidic protein, protein kinase C-α, and recoverin. RPCs expressed rhodopsin, a photoreceptor marker we never detected in MSCs. A majority of bone marrow derived-macrophages differentiated into cells that resembled microglia, rather than neural cells, in the explanted retina. This study shows that RPCs are likely to be a preferred cell type for retinal transplantation studies, compared with MSCs. However, MSCs may remain an attractive candidate for autologous transplantation. STEM CELLS *2006;24:2270–2278*

INTRODUCTION

Marrow stromal cells (MSCs) are a population of multipotent mesenchymal stem cells distinct from hematopoietic stem cells. MSCs were originally reported to contribute to the microenvironment of bone marrow and to be necessary for the proliferation of hematopoietic stem cells [1]. It has recently been shown that MSCs can differentiate into various cell lineages, including bone [2, 3], muscle [4], fat [5], cartilage [6], cardiomyocytes [7–9], and hepatocytes [10]. Recently, some studies claimed that MSCs could differentiate cells expressing markers of neurons and glia in vitro [11–17]. MSCs also have the capacity to migrate into the uninjured [18] and diseased brain [19, 20] and spinal cord [21, 22]. Interestingly, studies show that MSCs differentiate into cells expressing markers of photoreceptors and glia in the retina [23, 24].

The two major clinical subtypes of retinal degeneration (RD) are retinitis pigmentosa and age-related macular degeneration. A hallmark of these diseases is photoreceptor cell degeneration, resulting in visual loss. No effective restorative treatment exists for either RD subtype. Previously, we reported that brain-derived progenitor cells can migrate and differentiate into cells expressing markers of mature neurons and glia when grafted to the retina of mice and rats with RD [25–29]. Despite incorporation into the host retina and morphological similarities to various retinal cell types, the transplanted cells failed to express retina-specific markers in each of these studies. Recently, the transplantation of stem and progenitor cells isolated from retina has shown promise as a strategy for photoreceptor replacement [26, 28, 30–32]. Many mammalian tissues, including the retina, contain stem or progenitor cells that can be

Correspondence: Minoru Tomita, M.D., Ph.D., The Schepens Eye Research Institute, Department of Ophthalmology, Harvard Medical School, 20 Staniford St., Boston, Massachusetts 02114, USA. Telephone: 1-617-912-7419; Fax: 1-617-912-0101; e-mail: Minoru Tomita: tomita@vision.eri.harvard.edu; or Michael J. Young, Ph.D.: e-mail: mikey@vision.eri.harvard.edu Received October 12, 2005; accepted for publication May 23, 2006. 1066-5099/2006/$20.00/0 doi: 10.1634/stemcells.2005-0507.

isolated, propagated, and grafted into animal models of RD [26, 32]. The goal of retinal transplantation is the replacement of dead or diseased host cells with healthy, functional donor cells. In the present study, we investigated whether MSCs could effectively differentiate into retinal cells by using a cocktail of brain-derived neurotrophic factor (BDNF), nerve growth factor (NGF), and basic fibroblast growth factor (bFGF), which (as we previously reported) induces MSC differentiation into neurons [17]. Because there are reports of the differentiation of microglial cells into neurons [33] and bone marrow-derived macrophages into brain microglia [34, 35], we examined the differentiation of macrophages when grafted into the retina. Here, we compared the potential of retinal progenitor cells (RPCs) and MSCs for use in retinal transplantation studies.

Materials and Methods

Experimental Animals

All experiments were performed in adherence with the ARVO (Association for Research in Vision and Ophthalmology) Statement for the Use of Animals in Ophthalmic and Vision Research and with the Schepens Eye Research Institute Animal Care and Use Committee (Boston, MA). Rhodopsin knockout mice (rho−/− mice; C57/Bl6 background, provided by Peter Humphries, University of Dublin, Trinity College, Dublin, Ireland) and postnatal day 1 (P1) enhanced green fluorescence protein (EGFP) mice (C57BL/6 background; Dr. Masaru Okabe, University of Osaka, Osaka, Japan) were euthanized by CO_2 gas.

Isolation of MSCs and Macrophages

Humeri, femurs, and tibias were obtained from P1 EGFP mice and divided into small pieces. These small pieces were cultured in Dulbecco's modified Eagle's medium (DMEM)/F-12 with 10% fetal bovine serum (FBS), and the nonadherent cells were removed by replacement of the media. After approximately 2 weeks, the adherent cells became confluent and were incubated with trypsin for 3 minutes and removed from the flask. All cell cultures were maintained at 37°C, 5% CO_2.

After two or three passages, bone marrow-derived adherent cells were incubated with trypsin for 3 minutes to generate a single-cell suspension. Cells (1×10^6) were labeled with phycoerythrin-conjugated antibody against CD11b (1:50, marker for macrophages; BD Biosciences PharMingen, San Diego, http://www.bdbiosciences.com) and Cy-5-conjugated antibody against CD45 (1:50, marker for hematopoietic cells; BD Biosciences PharMingen). To isolate MSCs ($CD45^-$, $CD11b^-$) and macrophages ($CD45^+$, $CD11b^+$) from bone marrow-derived adherent cells, cell sorting was performed (data not shown). After sorting, the isolated MSCs and macrophages were cultured in 20% FBS for 2–3 days and then used for the subsequent experiments.

RPC Line

RPCs harvested from the retina of P1 EGFP mice were isolated and maintained in culture as previously described [32]. Briefly, retinas were surgically removed. The tissue was finely minced with two scalpel blades (no. 10), these whole retina homogenates were incubated in 0.1% collagenase, and a single-cell suspension was obtained. Dissociated cells were then cultured in DMEM/F-12 supplemented with B27 (Invitrogen, Carlsbad, CA, http://www.invitrogen.com) and 20 ng/ml of epidermal growth factor (EGF). The neurospheres that were generated could in turn be dissociated and subcultured to generate new spheres [26, 32].

Neural Differentiation and Characterization of MSCs

To examine the differentiation of GFP-expressing MSCs in vitro, MSCs were incubated with trypsin for 3 minutes to generate a single-cell suspension. Cells (1×10^3) were plated on eight-well poly(D-lysine)/laminin-coated chamber slides (BD Biosciences, San Jose, CA, http://www.bdbiosciences.com) in DMEM/F-12 medium supplemented with 25 ng/ml BDNF (R&D Systems, Minneapolis, http://www.rndsystems.com), 40 ng/ml NGF (R&D Systems), and 20 ng/ml bFGF (R&D Systems) and were fixed with 4% paraformaldehyde (PFA) at 2 weeks after plating. The cells were blocked in 1% bovine serum albumin (Sigma-Aldrich, St. Louis, http://www.sigmaaldrich.com) + 0.2% Triton-100 (Sigma-Aldrich) and then incubated for 2 hours with primary antibody to Ki67 (1:100, cell proliferation marker; Vector Laboratories, Burlingame, CA, http://www.vectorlabs.com), nestin (1:1, immature neuronal marker; Developmental Studies Hybridoma Bank, Iowa City, IA, http://www.uiowa.edu/~dshbwww/), glial fibrillary acidic protein (GFAP) (1:50, astrocyte marker, Dako), MAP-2 (1:500, neuronal markers; Sigma-Aldrich), anti-protein kinase C (PKC)-α (1:200, bipolar cell marker; Santa Cruz Biotechnology, Inc., Santa Cruz, CA, http://www.scbt.com), 2D4 rhodopsin (1:500, rod photoreceptor marker; kind gift of Dr. R. Molday, University of British Columbia, Vancouver, BC, Canada), and recoverin antibodies (1:1,000, photoreceptor and bipolar cell marker; Chemicon International, Temecula, CA, http://www.chemicon.com). After rinsing in phosphate-buffered saline (PBS [0.1 M]), samples were incubated in Cy3-conjugated species-specific IgG (1:800) for 1 hour. Samples were rinsed again and then coverslipped in polyvinyl alcohol-1,4-diazabicyclo (2.2.2) octane (PVA-Dabco) with 4′,6-diamidino-2-phenylindole (DAPI) and viewed under fluorescent illumination. As a control, the untreated MSCs were fixed with 4% PFA and labeled with the same antibodies.

Differentiation and Characterization of RPCs

To examine the differentiation of GFP-expressing RPCs in vitro, RPC spheres were incubated with trypsin for 1 minute to generate a single-cell suspension. In two separate experiments, cells (1×10^3) were plated on eight-well poly(D-lysine)/laminin-coated chamber slides (BD Biosciences) in DMEM/F-12 medium supplemented either with 10% FBS or with BDNF, NGF, and bFGF (the same growth factors used in MSCs differentiation experiments [17]) and were then fixed with 4% PFA at 1 day and 2 weeks after plating. The cells were then reacted and prepared with the antibodies described for MSCs.

Morphometry of Differentiated Cells

In each of the three culture conditions (MSCs with BDNF, NGF, and bFGF; RPCs with 10% FBS; and RPCs with BDNF, NGF, and bFGF), quantitative morphometry was performed by counting positive cells from a total cell number of at least 200 cells per well in randomly selected wells, selected based on DAPI

labeling (n = 5). In this counting study, cells (1×10^3) were plated on eight-well poly(D-lysine)/laminin-coated chamber slides (BD Biosciences). Five of eight wells were randomly chosen (by a masked observer), and all cells in the wells were counted. Nestin-positive cells from RPCs were counted at day 1, and MSCs and RPCs positive for other markers were counted after 2 weeks of treatment.

Reverse Transcription-Polymerase Chain Reaction Analysis of MSCs

For reverse transcription-polymerase chain reaction (RT-PCR) analysis, total RNA was extracted using TRIzol (Invitrogen) from MSCs grown in the presence or absence of BDNF, NGF, and bFGF in poly(D-lysine)/laminin-coated culture dishes (BD Biosciences) and from P1 EGFP mice retina for a positive control. First-strand cDNA was prepared from total RNA by reverse transcriptase using oligo(dT) primers. To detect nestin, β-tubulin class III (BT-III; neuronal marker), Map2, GFAP, PKC-α, recoverin, and rhodopsin, primers were used as described in Table 1.

Retinal Organ Culture

Retinal organ culture was performed as previously described [36–38] with minor modifications. Briefly, eyes were enucleated from rhodopsin knockout (rho−/−) mice and transferred to ice-cold Hanks' balanced salt solution (Invitrogen). The retinas were separated from the retinal pigment epithelium and placed onto Millicell-CM membrane culture inserts (diameter 30 mm, pore size 0.4 μm; Millipore Corporation, Billerica, MA, http://www.millipore.com) with the ganglion cell layer downward. The inserts with neural retina were placed in six-well plates containing approximately 1 ml/well of medium containing DMEM/F-12 supplemented with B27 neural supplement (Invitrogen), 2 mM L-glutamine (Sigma-Aldrich), 2,000 U of nystatin (Invitrogen), and 100 μl/ml penicillin-streptomycin (Sigma-Aldrich). Organ cultures were maintained at 37°C, 5% CO_2 and fed every 2–3 days.

Explant Coculture

The host retinas were explanted from rho−/− mice (4–8 weeks of age). Cell suspensions (1 μl, 5×10^3 cells/μl) containing (a) RPCs (n = 12); (b) MSCs with (n = 12) or without (n = 6) pretreatment with BDNF, NGF, and bFGF for 1 week; and (c) macrophages (n = 6) were added to the retinas using a pipette immediately after isolation of recipient retinas. We placed the grafted cells onto the surface of retinal explants using a 200-μl pipette. The cells were spread out over the entire surface of the explant, confirmed by viewing under fluorescent illumination. The explanted retinas were cultured for 1 week.

Tissue Preparation

After 1 week in explant coculture, the explanted retinas were fixed with 4% PFA, followed by cryoprotection with 20% sucrose. The retinas were sectioned at 12 μm on a cryostat. Sections were stained with neurofilament (NF) 200 (1:1,000, neuronal marker; Sigma-Aldrich), GFAP, PKC-α, recoverin, and rhodopsin antibodies as described above. After fixation with PFA and sucrose, some whole-mount retinas were stained with biotin-*Griffonia simplicifolia* (GS)-lectin (5 μg/ml, microglia and macrophages marker; Sigma-Aldrich) for 15 minutes and NF200 antibody for 2 hours. After rinsing in PBS, samples were respectively incubated in Cy3-conjugated streptavidin (Jackson ImmunoResearch Laboratories, Inc., West Grove, PA, http://www.jacksonimmuno.com) and Cy3-conjugated species-specific IgG (1:800) for 1 hour. Samples were rinsed again and then coverslipped in PVA-Dabco and viewed under fluorescent illumination.

RESULTS

Characterization of MSCs

When grown on conventional substrates in media supplemented with 10% FBS, GFP-transgenic MSCs exhibited high levels of endogenous green fluorescence (Fig. 1A). The untreated MSCs did not express nestin, Map2, GFAP, PKC-α, recoverin, or rhodopsin (data not shown). To examine differentiation in vitro, medium without 10% FBS was supplemented with BDNF, NGF, and bFGF. After 2 weeks of culture under differentiation conditions, MSCs differentiated into cells with neuronal morphologies and neurite-like processes (Fig. 1B) and also formed spheres (Fig. 1C). Subpopulations of MSCs expressed nestin (Fig. 1D–1F), Map2 (Fig. 1G–1I), GFAP (Fig. 1J–1L), PKC-α (Fig. 1M–1O), and recoverin (Fig. 1P–1R). These markers are consistent, although not conclusive, with differentiation into

Table 1. Primers used for reverse transcription-polymerase chain reaction analysis

Genes	Primer sequences (5′–3′)	Product size (bp)	Temperature (°C)
Nestin	F: AACTGGCACACCTCAAGATGT R: TCAAGGGTATTAGGCAAGGGG	235	60
GFAP	F: CACGAACGAGTCCCTAGAGC R: ATGGTGATGCGGTTTTCTTC	234	60
TB-III	F: ACCTCAACCACCTGGTATCG R: TGCTGTTCTTGCTCTGGATG	344	60
Map2	F: CTGGACATCAGCCTCACTCA R:AATAGGTGCCCTGTGACCTG	164	60
PKC-α	F: CCCATTCCAGAAGGAGATGA R: TTCCTGTCAGCAAGCATCAC	212	60
Recoverin	F: ATGGGGAATAGCAAGAGCGG R: GAGTCCGGGAAAAACTTGGAATA	179	60
Rhodopsin	F: TCACCACCACCCTCTACACA R: TGATCCAGGTGAAGACCACA	216	60

Abbreviations: bp, base pair; F, forward; GFAP, glial fibrillary acidic protein; PKC, protein kinase C; R, reverse; TB, tubulin.

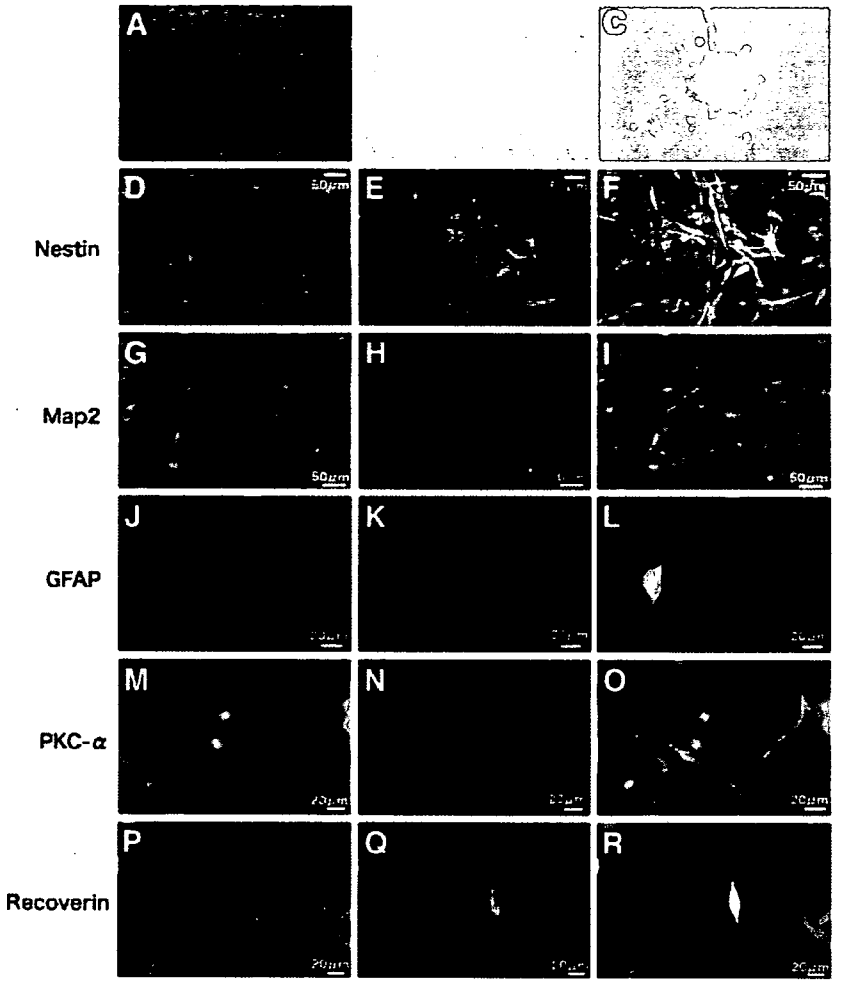

Figure 1. Differentiation and characterization of marrow stromal cell (MSCs) in vitro. Undifferentiated GFP$^+$ MSCs grown in Dulbecco's modified Eagle's medium with 10% fetal bovine serum, viewed under fluorescein isothiocyanate illumination (**A**). MSCs cultured in serum-free medium with brain-derived neurotrophic factor, nerve growth factor, and basic fibroblast growth factor for 14 days (**B–R**). After 2 weeks of culture under differentiation conditions, MSCs morphologically differentiated into neuronal shape and had neuronal processes (**B**) and also formed spheres (**C**). Constitutive GFP expression (**D, G, J, M, P**), antibody/cytokeratin-3 immunoreactivity for nestin (**E**), Map2 (**H**), GFAP (**K**), PKC-α (**N**), and recoverin (**Q**), and merged images (**F, I, L, O, R**). Abbreviations: GFAP, glial fibrillary acidic protein; GFP, green fluorescent protein; PKC, protein kinase C.

retinal neurons. Interestingly, these immunopositive cells also showed morphological evidence suggestive of differentiation into immature photoreceptors, bipolar cell types, glial cells, and neuronal cells (Fig. 1F, 1I, 1L, 1O, 1R). We could not find any rhodopsin-positive cells from treated MSCs.

Characterization of RPCs

When grown on conventional substrates in medium supplemented with EGF, GFP-transgenic RPCs exhibited high levels of endogenous green fluorescence (Fig. 2A) and maintained an undifferentiated state characterized by ubiquitous Ki67 and nestin immunoreactivity (Fig. 2B, 2C). Cells could be maintained in this state for up to 1 year or 50 passages as neurospheres. To examine differentiation in vitro, medium without EGF was supplemented with 10% FBS. After 2 weeks culture under differentiation conditions, the cells were analyzed immunocytochemically. The number of Ki67$^+$ cells markedly decreased (data not shown), and subpopulations expressed GFAP (Fig. 2D), Map2 (Fig. 2E), PKC-α (Fig. 2F), recoverin (Fig. 2G), or rhodopsin (Fig. 2H). These markers are consistent with differentiation into rod photoreceptors, bipolar cells, and Muller glia, all of which are known to be born late in retinogenesis. Moreover, these immunopositive cells also showed morphological evidence suggestive of immature photoreceptor differentiation, as well as of other retinal cell types (Fig. 2D–2H).

Quantitative Evaluation of Differentiated Cell Numbers: MSCs Versus RPCs

To examine the optimal source of cells for retinal transplantation, quantitative evaluation of differentiation into neuronal and retinal cells was carried out using cell counting as previously described [39].

After 2 weeks of BDNF, NGF, and bFGF treatment, the percentages of surviving MSCs expressing nestin, Map2, GFAP, PKC-α, and recoverin were 5.55%, 3.27%, 1.42%, 3.97%, and 13.9%, respectively. The percentages of nestin-, Map2-, GFAP-, PKC-α-, recoverin-, and rhodopsin-positive cells from RPCs treated with 10% FBS were 90.5%, 15.2%, 64.4%, 12.9%, 23.6%, and 3.17%, respectively. The rates of nestin-, Map2-, GFAP-, PKC-α-, recoverin-, and rhodopsin-positive cells from RPCs treated with BDNF, NGF, and bFGF were 89.2%, 29.4%, 10.9%, 28.2%, 22.3%, and 2.25%, respectively (Fig. 3A).

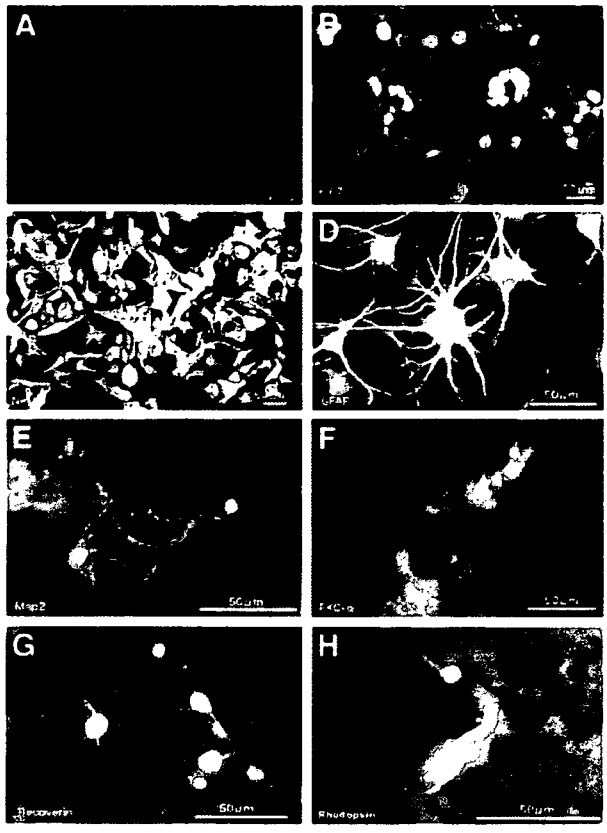

Figure 2. Differentiation and characterization of retinal progenitor cell (RPCs) in vitro. RPCs formed green fluorescent protein-positive neurospheres (**A**). RPCs cultured in the absence of epidermal growth factor and in the presence of 10% fetal bovine serum for 1 (**B, C**) or 14 (**D–H**) days. The cells were stained for Ki67 (**B**), nestin (**C**), GFAP (**D**), Map2 (**E**), PKC-α (**F**), recoverin (**G**), and rhodopsin (**H**). Abbreviations: GFAP, glial fibrillary acidic protein; MSC, marrow stromal cell; PKC, protein kinase C.

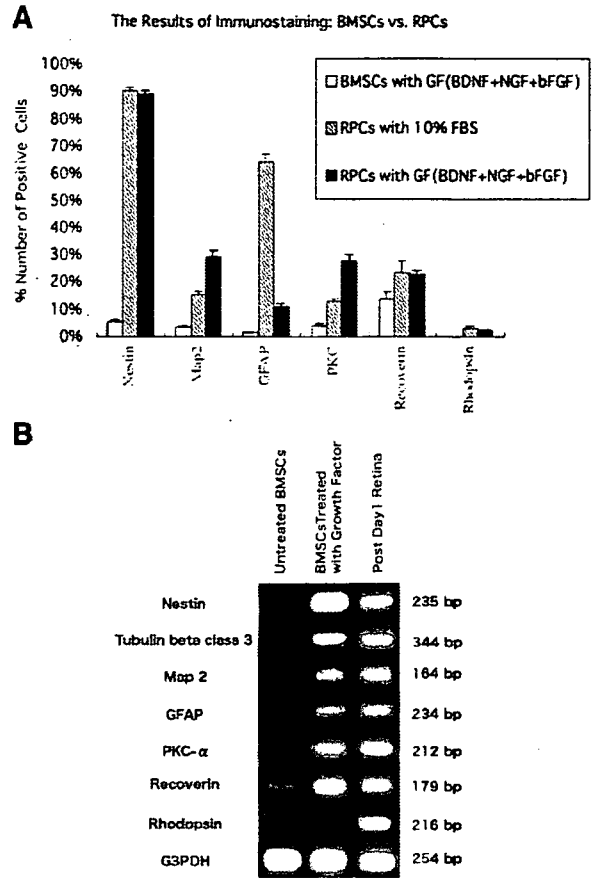

Figure 3. Comparison of BMSCs and RPCs. (**A**): The number of cells differentiated into retinal cells: comparison of marrow stromal cell (MSCs) and RPCs. In this study, nestin-positive cells were counted at day 1, and other markers cells were counted at 2 weeks after treatment. (**B**): Effect of BDNF, NGF, and bFGF on transcription of retinal cell markers. Semiquantitative reverse transcription-polymerase chain reaction analysis was carried out to determine the effect of BDNF, NGF, and bFGF on MSCs. MSCs without treatment showed only weak recoverin expression. (MSCs without treatment did not express nestin, BT-III, Map2, GFAP, PKC-α, and rhodopsin completely.) After 2 weeks of BDNF, NGF, and bFGF treatment, treated MSCs expressed nestin, BT-III, Map2, GFAP, PKC-α, and recoverin; however, rhodopsin expression was not found. Recoverin expression was increased in treated MSCs. Abbreviations: BDNF, brain-derived neurotrophic factor; bFGF, basic fibroblast growth factor; BMSC, bone marrow stromal cell; bp, base pair; BT-III, β-tubulin class III; FBS, fetal bovine serum; GF, growth factor; GFAP, glial fibrillary acidic protein; NGF, nerve growth factor; PKC, protein kinase C; RPC, retinal progenitor cell.

RT-PCR Analysis of BDNF, NGF, and bFGF Treatment

Semiquantitative RT-PCR analysis was carried out to determine the effect of BDNF, NGF, and bFGF on MSCs (Fig. 3B). MSCs without treatment showed only weak recoverin expression. (MSCs without treatment did not express nestin, BT-III, Map2, GFAP, PKC-α, or rhodopsin.) After 2 weeks of BDNF, NGF, and bFGF treatment, MSCs expressed nestin, BT-III, Map2, GFAP, PKC-α, and recoverin. Rhodopsin expression was not found. Recoverin expression was increased in treated MSCs.

Macrophages Differentiated into Microglia After Coculture with Explanted Retinas

After coculture with explanted rho−/− mouse retinas, macrophages were viewed by fluorescent illumination at 3 and 7 days. Macrophages migrated into the retina and assumed morphology very reminiscent of microglial cells (Fig. 4A–4C). The cocultured macrophages also expressed GS-lectin, a marker of microglia (Fig. 4D–4F). There was no evidence of neuronal differentiation upon immunocytochemical and morphological analyses (data not shown).

Migration and Differentiation of MSCs

At 1 week in coculture, MSCs with and without pretreatment of BDNF, NGF, and bFGF migrated into explanted rho−/− retina (Fig. 5A). MSCs without pretreatment did not show morphological or immunocytochemical evidence of neural differentiation (data not shown). On the other hand, pretreated MSCs showed morphological and immunocytochemical evidence of neuronal differentiation. Pretreated MSCs migrated into explanted retinas (Fig. 5A) and expressed NF200 (Fig. 5B–5G), GFAP (Fig. 5H–5J), PKC-α (Fig. 5K–5M), and recoverin (Fig.

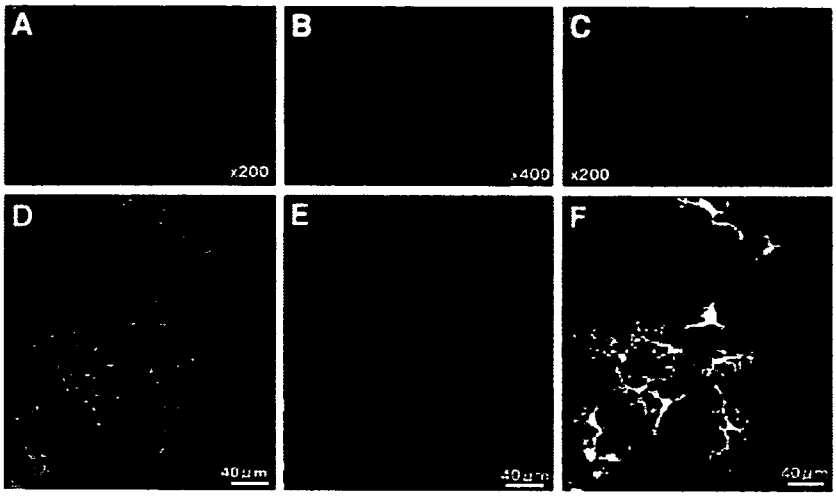

Figure 4. Macrophages differentiated into microglia after transplantation to explanted retinas. Rho−/− mice retina at 3 (**A**) and 7 (**B, C**) days. Macrophages migrated into retina and morphologically changed their shape to that resembling microglia (**A–C**). Confocal (**D–F**) images seen at 1 week after grafting; constitutive green fluorescent protein expression (**D**), macrophage/microglia antibody/cytokeratin-3 immunoreactivity (**E**), and merged images (**F**).

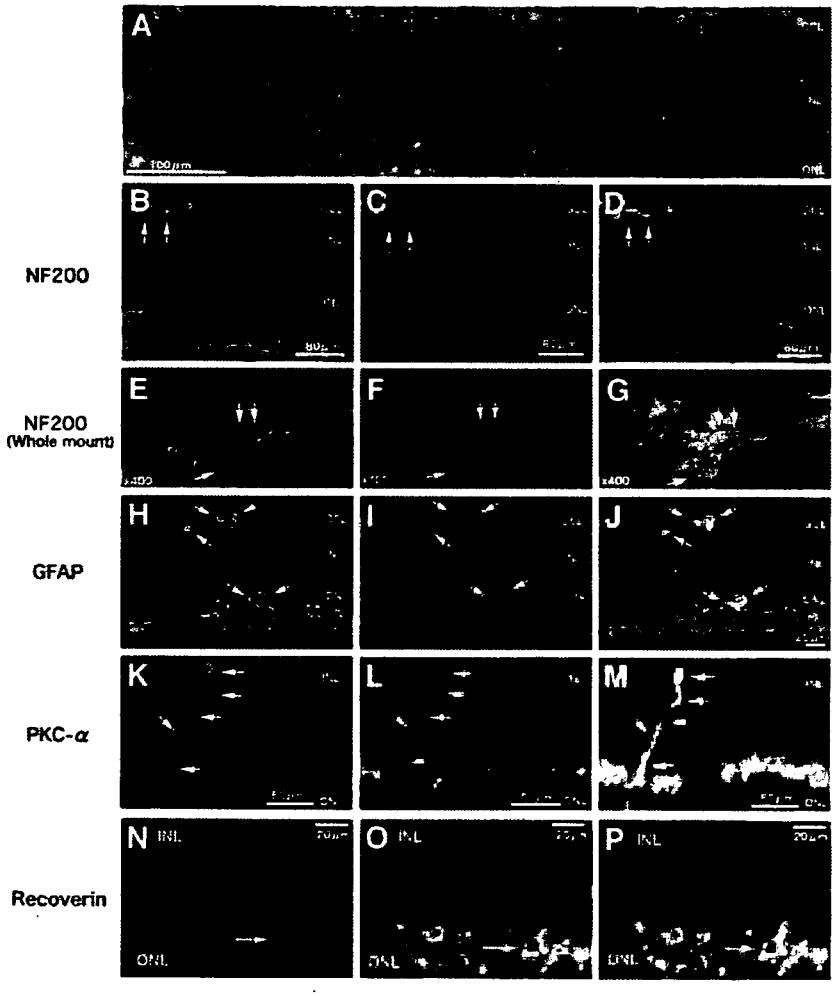

Figure 5. Migration and differentiation of pretreated marrow stromal cell (MSCs) into explanted retinas of rho−/− mice. A large number of MSCs migrated into explanted retinas of rho−/− mice (**A**). Epi-fluorescent (**K–P**) and confocal (**B–J**) images of the expression of neural and photoreceptor markers by pretreated MSCs that were grafted onto explanted retinas from rho−/− mice, seen at 1 week after grafting; constitutive green fluorescent protein expression (**B, E, H, K, N**), antibody/cytokeratin-3 immunoreactivity for NF200 (**C, F**) (whole mount), GFAP (**I**), PKC-α (**L**), recoverin (**O**), and merged images (**D, G, J, M, P**). Abbreviations: GCL, ganglion cell layer; GFAP, glial fibrillary acidic protein; INL, inner nuclear layer; NF, neurofilament; ONL, outer nuclear layer; PKC, protein kinase C.

5N–5P). We also found morphological evidence of neuronal differentiation (Fig. 5B–5P). However, we could not find any rhodopsin-positive cells among coculture, pretreated MSCs.

Migration and Differentiation of RPCs

At 1 week in coculture, RPCs migrated into all retinal lamina adjacent to the graft after addition to the outer retina and showed

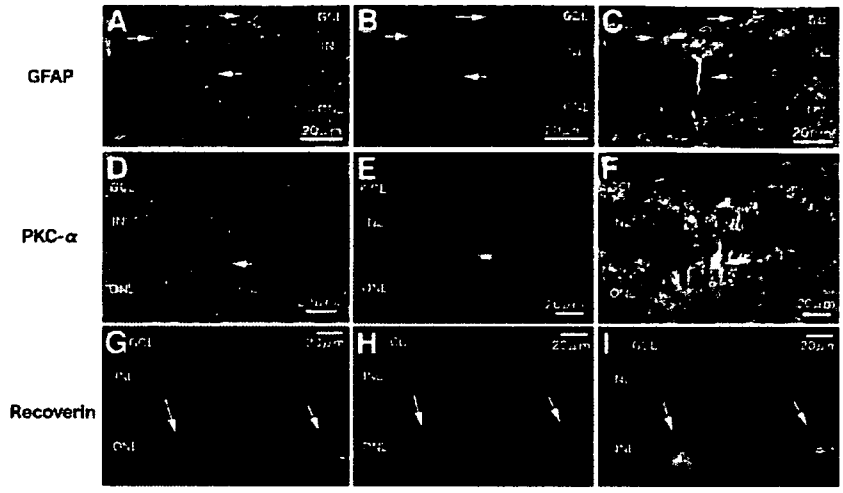

Figure 6. Migration and differentiation of pretreated retinal progenitor cells (RPCs) into explanted retinas of rho−/− mice. Confocal images of the expression of neural and photoreceptor markers by RPCs grafting to explanted retinas of rho−/− mice, seen at 1 week after grafting: constitutive green fluorescent protein expression (**A, D, G**), antibody/cytokeratin-3 immunoreactivity for GFAP (**B**), PKC-α (**E**), recoverin (**H**), and merged images (**C, F, I**). Abbreviations: GCL, ganglion cell layer; GFAP, glial fibrillary acidic protein; INL, inner nuclear layer; MSC, marrow stromal cell; ONL, outer nuclear layer; PKC, protein kinase C.

morphological evidence of neuronal differentiation (Fig. 6D–6I). GFP^+ donor cells coexpressed a number of markers indicative of phenotypic maturation, including GFAP (Fig. 6A–6C), PKC-α (Fig. 6D–6F), and recoverin (Fig. 6G–6I). In the rho−/− mice, the rod marker rhodopsin was not detected in either grafted RPCs or the host outer nuclear layer.

Discussion

The results presented here demonstrate that MSCs treated with BDNF, NGF, and bFGF can differentiate into retinal cells expressing Map2. BT-III, GFAP, PKC-α, and recoverin by immunocytochemistry and RT-PCR. In the explanted retina, pretreated MSCs showed differentiation into retinal cells expressing NF200, GFAP, PKC-α, and recoverin, although nonpretreated MSCs did not show any evidence of differentiation into retinal cells. This shows that treatment with growth factors (as in our previous report [17]) is very important for neural induction of MSCs. Moreover, our data show that using growth factors promoted neuronal differentiation over glial differentiation in RPCs (Fig. 3A). In the present study, RPCs clearly showed a higher level of differentiation into retinal cells compared with MSCs. Induced MSCs expressed neuronal and glial markers and morphologically differentiated into neuron- and glia-like cells; however, RPCs showed better morphological differentiation and also expressed rhodopsin (Figs. 1, 2). Although a subpopulation of MSCs differentiated morphologically into neuronal-like cells and expressed neuronal markers, the majority remained undifferentiated both in terms of morphology and marker expression during the time course examined. The lack of rhodopsin expression in vivo and in vitro by MSCs may be an impediment to their use in photoreceptor replacement. One must be cognizant of the fact that the absence of evidence is not evidence of absence. The lack of differentiation in vitro indicates that the optimal conditions have yet to be determined. This is especially true in the case of RPC photoreceptor differentiation, which we have shown to be dependent upon specific conditions in vivo. The fact that RPCs failed to express rhodopsin after migration into explants is not surprising, considering that our previous studies found no evidence for rhodopsin among RPCs transplanted to rho−/− mice in vivo [32]. The same study showed that RPCs expressed rhodopsin in another mouse strain with RD, the C3H mouse [32].

As with previous studies in the brain [34, 35], our results showed that macrophages migrated into explanted retina and appeared to differentiate into microglia. Although a previous report showed that microglia have potential for neuronal differentiation [33], we did not find evidence of differentiation into neuronal or glial cells in our explant study. Further studies will be needed to determine the neuronal potential of macrophages and microglia.

From a clinical perspective, MSCs are a good source for stem cell transplantation. Bone marrow cell transplantation is already an approved therapy for some kinds of hematological diseases and has the advantage of the possibility of autologous cell transplantation. Moreover, because recent reports have shown that MSCs have the capacity to modulate allogeneic cellular immunity [40, 41], MSCs may be useful for allogeneic transplantation.

Cell fusion has recently been proposed as the underlying explanation for the apparent plasticity and "transdifferentiation" of stem cells, including MSCs. This raises questions about the mechanisms of transdifferentiation in vitro and in vivo [42, 43]. Evidence against cell fusion has begun to mount; recent studies reported that MSCs can undergo transdifferentiation into various organ cell types, including neurons, without fusion [10, 44, 45]. We believe that our results cannot be attributed to cell fusion; this study shows that MSC differentiation into post-mitotic neuronal and retinal cells occurred in a controlled culture environment. Recent studies have shown that MSCs have a potential of transdifferentiation as cultured MSCs express mesodermal, endodermal, ectodermal, and germline genes, suggesting the potential to differentiate into all these cell types [46–48]. Moreover, our previous study [17], using the same methods for neuronal induction as this study, showed neuroectodermal induction, neural differentiation, and calcium uptake in response to a depolarizing stimulus from human MSCs. It has also been reported that neuroectodermal induction and electrophysiological characteristics of midbrain dopaminergic, serotonergic, and GABA-ergic neurons arise from treated MSCs [16].

CONCLUSION

The present study shows that RPCs have clear advantages over MSCs in potential retinal transplantation applications. First, no evidence was found for MSC differentiation into rod photoreceptors. Second, RPCs showed more complete differentiation into retinal cell subtypes than did MSCs, and this occurred at a significantly higher rate. Finally, we have previously reported that neuronal progenitor cells (NPCs) have inherent immune privilege, suggesting increased resistance of allogeneic NPC grafts to host rejection [49, 50]. Such findings suggest the possibility that RPCs possess immune privilege properties as well. MSCs also have significant therapeutic potential in transplantation medicine because they can be readily obtained through a well-established clinical procedure. They are relatively easy to isolate and expand for autologous transplantation without the need for immunosuppression or the risk of rejection. In this comparison study, we submit that RPCs possess significant advantages for differentiation into retinal cells compared with MSCs.

ACKNOWLEDGMENTS

This work was supported by grants from the U.S. Department of Defense, National Institutes of Health (09595; M.J.Y.), and by a gift from Richard and Gail Siegal. We thank Prof. Susumu Ikehara (Department of Pathology, Kansai Medical University, Osaka, Japan) for advice.

DISCLOSURES

The authors indicate no potential conflicts of interest.

REFERENCES

1 Dexter TM, Allen TD, Lajtha LG. Conditions controlling the proliferation of haemopoietic stem cells in vitro. J Cell Physiol 1977;91:335–344.

2 Rickard DJ, Sullivan TA, Shenker BJ et al. Induction of rapid osteoblast differentiation in rat bone marrow stromal cell cultures by dexamethasone and BMP-2. Dev Biol 1994;161:218–228.

3 Tsuchiya K, Mori T, Chen G et al. Custom-shaping system for bone regeneration by seeding marrow stromal cells onto a web-like biodegradable hybrid sheet. Cell Tissue Res 2004;316:141–153.

4 Ferrari G, Cusella-De Angelis G, Coletta M et al. Muscle regeneration by bone marrow-derived myogenic progenitors. Science 1998;279: 1528–1530.

5 Umezawa A, Tachibana K, Harigaya K et al. Colony-stimulating factor 1 expression is down-regulated during the adipocyte differentiation of H-1/A marrow stromal cells and induced by cachectin/tumor necrosis factor. Mol Cell Biol 1991;11:920–927.

6 Ashton BA, Allen TD, Howlett CR et al. Formation of bone and cartilage by marrow stromal cells in diffusion chambers in vivo. Clin Orthop Relat Res 1980;151:294–307.

7 Orlic D, Kajstura J, Chimenti S et al. Bone marrow cells regenerate infarcted myocardium. Nature 2001;410:701–705.

8 Takeda Y, Mori T, Imabayashi H et al. Can the life span of human marrow stromal cells be prolonged by bmi-1, E6, E7, and/or telomerase without affecting cardiomyogenic differentiation? J Gene Med 2004;6: 833–845.

9 Makino S, Fukuda K, Miyoshi S et al. Cardiomyocytes can be generated from marrow stromal cells in vitro. J Clin Invest 1999;103:697–705.

10 Sato Y, Araki H, Kato J et al. Human mesenchymal stem cells xenografted directly to rat liver differentiated into human hepatocytes without fusion. Blood 2005;106:756–763.

11 Woodbury D, Schwarz EJ, Prockop DJ et al. Adult rat and human bone marrow stromal cells differentiate into neurons. J Neurosci Res 2000; 61:364–370.

12 Kohyama J, Abe H, Shimazaki T et al. Brain from bone: Efficient "meta-differentiation" of marrow stroma-derived mature osteoblasts to neurons with Noggin or a demethylating agent. Differentiation 2001;68: 235–244.

13 Suzuki H, Taguchi T, Tanaka H et al. Neurospheres induced from bone marrow stromal cells are multipotent for differentiation into neuron, astrocyte, and oligodendrocyte phenotypes. Biochem Biophys Res Commun 2004;322:918–922.

14 Sanchez-Ramos J, Song S, Cardozo-Pelaez F et al. Adult bone marrow stromal cells differentiate into neural cells in vitro. Exp Neurol 2000; 164:247–256.

15 Neuhuber B, Gallo G, Howard L et al. Reevaluation of in vitro differentiation protocols for bone marrow stromal cells: Disruption of actin cytoskeleton induces rapid morphological changes and mimics neuronal phenotype. J Neurosci Res 2004;77:192–204.

16 Jiang Y, Henderson D, Blackstad M et al. Neuroectodermal differentiation from mouse multipotent adult progenitor cells. Proc Natl Acad Sci U S A 2003;100:11854–11860.

17 Mori T, Kiyono T, Imabayashi H et al. Combination of hTERT and bmi-1, E6, or E7 induces prolongation of the life span of bone marrow stromal cells from an elderly donor without affecting their neurogenic potential. Mol Cell Biol 2005;25:5183–5195.

18 Kopen GC, Prockop DJ, Phinney DG. Marrow stromal cells migrate throughout forebrain and cerebellum, and they differentiate into astrocytes after injection into neonatal mouse brains. Proc Natl Acad Sci U S A 1999;96:10711–10716.

19 Chopp M, Li Y. Treatment of neural injury with marrow stromal cells. Lancet Neurol 2002;1:92–100.

20 Dezawa M, Kanno H, Hoshino M et al. Specific induction of neuronal cells from bone marrow stromal cells and application for autologous transplantation. J Clin Invest 2004;113:1701–1710.

21 Akiyama Y, Radtke C, Honmou O et al. Remyelination of the spinal cord following intravenous delivery of bone marrow cells. Glia 2002; 39:229–236.

22 Hofstetter CP, Schwarz EJ, Hess D et al. Marrow stromal cells form guiding strands in the injured spinal cord and promote recovery. Proc Natl Acad Sci U S A 2002;99:2199–2204.

23 Tomita M, Adachi Y, Yamada H et al. Bone marrow-derived stem cells can differentiate into retinal cells in injured rat retina. STEM CELLS 2002;20:279–283.

24 Kicic A, Shen WY, Wilson AS et al. Differentiation of marrow stromal cells into photoreceptors in the rat eye. J Neurosci 2003;23:7742–7749.

25 Mizumoto H, Mizumoto K, Shatos MA et al. Retinal transplantation of neural progenitor cells derived from the brain of GFP transgenic mice. Vision Res 2003;43:1699–1708.

26 Klassen H, Sakaguchi DS, Young MJ. Stem cells and retinal repair. Prog Retin Eye Res 2004;23:149–181.

27 Young MJ, Ray J, Whiteley SJ et al. Neuronal differentiation and morphological integration of hippocampal progenitor cells transplanted to the retina of immature and mature dystrophic rats. Mol Cell Neurosci 2000;16:197–205.

28 Klassen H, Ziaeian B, Kirov II et al. Isolation of retinal progenitor cells from post-mortem human tissue and comparison with autologous brain progenitors. J Neurosci Res 2004;77:334–343.

29 Lu B, Kwan T, Kurimoto Y et al. Transplantation of EGF-responsive neurospheres from GFP transgenic mice into the eyes of rd mice. Brain Res 2002;943:292–300.

30 Ahmad I, Dooley CM, Thoreson WB et al. In vitro analysis of a mammalian retinal progenitor that gives rise to neurons and glia. Brain Res 1999;831:1–10.

31 Tropepe V, Coles BL, Chiasson BJ et al. Retinal stem cells in the adult mammalian eye. Science 2000;287:2032–2036.

32 Klassen HJ, Ng TF, Kurimoto Y et al. Multipotent retinal progenitors express developmental markers, differentiate into retinal neurons, and preserve light-mediated behavior. Invest Ophthalmol Vis Sci 2004;45: 4167–4173.

33 Yokoyama A, Yang L, Itoh S et al. Microglia, a potential source of neurons, astrocytes, and oligodendrocytes. Glia 2004;45:96–104.

34 Tanaka R, Komine-Kobayashi M, Mochizuki H et al. Migration of enhanced green fluorescent protein expressing bone marrow-derived microglia/macrophage into the mouse brain following permanent focal ischemia. Neuroscience 2003;117:531–539.

35 Eglitis MA, Mezey E. Hematopoietic cells differentiate into both microglia and macroglia in the brains of adult mice. Proc Natl Acad Sci U S A 1997;94:4080–4085.

36 Zhang Y, Caffe AR, Azadi S et al. Neuronal integration in an abutting-retinas culture system. Invest Ophthalmol Vis Sci 2003;44:4936–4946.

37 Zhang Y, Kardaszewska AK, van Veen T et al. Integration between abutting retinas: Role of glial structures and associated molecules at the interface. Invest Ophthalmol Vis Sci 2004;45:4440–4449.

38 Akita J, Takahashi M, Hojo M et al. Neuronal differentiation of adult rat hippocampus-derived neural stem cells transplanted into embryonic rat explanted retinas with retinoic acid pretreatment. Brain Res 2002;954: 286–293.

39 Zahir T, Klassen H, Young MJ. Effects of ciliary neurotrophic factor on differentiation of late retinal progenitor cells. STEM CELLS 2005;23: 424–432.

40 Aggarwal S, Pittenger MF. Human mesenchymal stem cells modulate allogeneic immune cell responses. Blood 2005;105:1815–1822.

41 Beyth S, Borovsky Z, Mevorach D et al. Human mesenchymal stem cells alter antigen-presenting cell maturation and induce T-cell unresponsiveness. Blood 2005;105:2214–2219.

42 Alvarez-Dolado M, Pardal R, Garcia-Verdugo JM et al. Fusion of bone-marrow-derived cells with Purkinje neurons, cardiomyocytes and hepatocytes. Nature 2003;425:968–973.

43 Weimann JM, Johansson CB, Trejo A et al. Stable reprogrammed heterokaryons form spontaneously in Purkinje neurons after bone marrow transplant. Nat Cell Biol 2003;5:959–966.

44 Pochampally RR, Neville BT, Schwarz EJ et al. Rat adult stem cells (marrow stromal cells) engraft and differentiate in chick embryos without evidence of cell fusion. Proc Natl Acad Sci U S A 2004;101:9282–9285.

45 Cogle CR, Yachnis AT, Laywell ED et al. Bone marrow transdifferentiation in brain after transplantation: A retrospective study. Lancet 2004; 363:1432–1437.

46 Tremain N, Korkko J, Ibberson D et al. MicroSAGE analysis of 2,353 expressed genes in a single cell-derived colony of undifferentiated human mesenchymal stem cells reveals mRNAs of multiple cell lineages. STEM CELLS 2001;19:408–418.

47 Seshi B, Kumar S, King D. Multilineage gene expression in human bone marrow stromal cells as evidenced by single-cell microarray analysis. Blood Cells Mol Dis 2003;31:268–285.

48 Woodbury D, Reynolds K, Black IB. Adult bone marrow stromal stem cells express germline, ectodermal, endodermal, and mesodermal genes prior to neurogenesis. J Neurosci Res 2002;69:908–917.

49 Hori J, Ng TF, Shatos M et al. Neural progenitor cells lack immunogenicity and resist destruction as allografts. STEM CELLS 2003; 21:405–416.

50 Klassen H, Imfeld KL, Ray J et al. The immunological properties of adult hippocampal progenitor cells. Vision Res 2003;43:947–956.

JOURNAL OF CELLULAR PHYSIOLOGY 208:188–194 (2006)

Increased Mobilization of c-kit$^+$ Sca-1$^+$ Lin$^-$ (KSL) Cells and Colony-Forming Units in Spleen (CFU-S) Following De Novo Formation of a Stem Cell Niche Depends on Dynamic, But Not Stable, Membranous Ossification

KAZUNARI NAGAYOSHI,[1,2] HIROYUKI OHKAWA,[2] KEIGO YOROZU,[2] MASATO HIGUCHI,[2] SAYUMI HIGASHI,[2] NAOKI KUBOTA,[2] HIROYASU FUKUI,[2] NOBUO IMAI,[2] SATOSHI GOJO,[3] JUN-ICHI HATA,[1] YOSHIRO KOBAYASHI,[4] AND AKIHIRO UMEZAWA[1]*

[1]*Department of Reproductive Biology and Pathology, National Research Institute for Child Health and Development, Tokyo, Japan*

[2]*Chugai Pharmaceutical Co., LTD, Fuji Gotemba Research Institute, Gotemba, Shizuoka, Japan*

[3]*Department of Cardiovascular Surgery, Saitama Medical Center, Kawagoe, Japan*

[4]*Department of Biomolecular Science, Faculty of Science, Toho University, Chiba, Japan*

Stem cells are thought to inhabit in a unique microenvironment, known as "niche," in which they undergo asymmetric cell divisions that results in reproducing both stem cells and progenies to maintain various tissues throughout life. The cells of osteoblastic lineage have been identified as a key participant in regulating the number of hematopoietic stem cells (HSCs). HSCs receive their regulatory messages from the microenvironment in the bone marrow. This would account for a reason why the localization of hematopoiesis is usually restricted in the bone marrow. To clarify the above possibility we employed a cell implantation-based strategy with a unique osteoblast cell line (KUSA-A1) derived from a C3H/He mouse. The implantation of KUSA-A 1 cells resulted in the generation of ectopic bones in the subcutaneous tissues of the athymic BALB/c nu/nu mice. Subsequently the mice obtained a greater amount of the bone marrow than normal mice, and they showed an increased number of HSCs. These results indicate that the newly generated osteoblasts-derived ectopic bones are responsible for the increase in the number of the HSC population. Furthermore, the increased number of HSCs directly correlates with both the magnitude of dynamic osteogenic process and the size of the newly generated bone or "niche." J. Cell. Physiol. 208: 188–194, 2006. © 2006 Wiley-Liss, Inc.

Stem cell with potential for self-renewal and multilineage differentiation can be identified in various self-renewing tissues, including epidermis, intestinal epithelium, and testis, and hematopoietic stem cells (HSCs) are also capable of both self-renewal and multipotency (Ikehara, 2000; Weissman, 2000). The most important experimental evidence for the existence of such cells is the ability of a single bone-marrow-derived cell to reconstitute long-term hematopoiesis in lethally irradiated recipients (Till and McCulloch, 1961; Siminovitch et al., 1963; Till et al., 1964; Matsuzaki et al., 2004). Molecular markers that characterize transplantable cells with stem cell potential and allow their selective purification have been identified, and this achievement has been important to progress both applied and basic science (Spangrude et al., 1988; Goodell et al., 1996). As an example, CD34$^-$, c-kit$^+$, Sca-1$^+$, and Lin$^-$ cells have been identified as the most primitive HSCs (Osawa et al., 1996).

Stem-cell fate decisions in the developing embryo are governed by complex interplays between cell-autonomous signals and stimuli from the surrounding tissues. Stem cells are thought to inhabit in a unique microenvironment, known as "niche," in which they undergo asymmetric divisions that generate both stem cells and progenies to maintain the tissue throughout life (Dzierzak et al., 1998; Matsuzaki et al., 2004). HSCs migrate from the yolk sac to the liver during early development, and they ultimately settle in the bone marrow and spleen of the adult. The bone marrow and spleen serve as the microenvironment that supports the HSCs via cytokines, membrane-bound molecules, and gap junctions. And the classical experiment on HSC-colony formation by Till and McCulloch (1961) showed that reconstitution of hematopoiesis takes place only in hematopoietic organs. The niche hypothesis was first proposed by Schöfield, 1978, and it is supported by the evidence that HSCs have been successfully maintained in co-culture systems with marrow-derived stromal cells in vitro. Steel mice (Sl/Sld) have a mutation at the Sl locus, and spleen colonies cannot be produced in the mice when transplanted with normal marrow cells.

This article includes Supplementary Material available from the authors upon request or via the Internet at http://www.interscience.wiley.com/jpages/0021-9541/suppmat.

Contract grant sponsor: Ministry of Education, Culture, Sports, Science, and Technology (MEXT) of Japan; Contract grant numbers: 14081208, 13470053, 14657051); Contract grant sponsor: Health and Labour Sciences Research Grants; Contract grant numbers: H-14-trans-003, KH71064; Contract grant sponsor: Pharmaceuticals and Medical Devices Agency; Contract grant number: 02-2.

*Correspondence to: Akihiro Umezawa, Department of Reproductive Biology and Pathology, National Research Institute for Child Health and Development, 2-10-1 Okura, Setagaya-ku, Tokyo 157-8535, Japan. E-mail: umezawa@1985.jukuin.keio.ac.jp

Received 26 July 2005; Accepted 13 February 2006

DOI: 10.1002/jcp.20652

Steel mice have a defect in the hematopoietic microenvironment, or the niche, where marrow stromal cells constitute (Harrison and Russell, 1972).

Bone marrow stromal cells are capable of differentiating into adipocytes, endothelial cells, chondrocytes, and osteoblasts (Pittenger et al., 1999). They are also capable of transdifferentiating into cardiomyocytes, skeletal myocytes, and neurons when exposed to inducers in vitro and in vivo (Umezawa et al., 1992; Makino et al., 1999; Kohyama et al., 2001; Takeda et al., 2004; Mori et al., 2005; Terai et al., 2005). Previous studies on the role of stromal cells in supporting HSCs have mainly been based on in vitro culture. The trabecular area of cancellous bone is the primary site of HSCs. They arise next to the inner surface of bone, and then migrate towards the blood vessels at the center of the bone marrow cavity as they mature. Since the 1970s, efforts to characterize the HSC niche have been focusing on developing systems in vitro that mimic some of the features of stem cell–niche interactions in vivo, and single clones of stromal cells have been found to be capable of supporting HSC self-renewal and differentiation in vivo (Okada et al., 1991, 1992). Osteoblastic marrow stromal cells are a regulatory component of the HSC niche in vivo that influences stem cell function, and some stromal cell clones are part of the bone-forming 'osteoblastic' lineage, which is consistent with a notion that osteoblasts may be a component of the HSC niche in vivo (Lord, 1990; Yoshimoto et al., 2003).

In the present study, we demonstrate that KUSA-A1 osteoblasts, whose number has been increased by local injection into the tissues, support an increase in the number of HSCs in both bone marrow and peripheral blood as a result of an increase in size of the microenvironment or niche in vivo. We provide in vivo evidence that shows an extra osteogenic process independent from that in the normal bone affects the reproduction of stem cells.

MATERIALS AND METHODS

Mice and their major histocompatibility complex (MHC) Class I

BALB/c nu/nu (H-2d), BALB/c (H-2d), C57BL/6N (H-2b), and C3H/He (H-2k) mice were obtained from Clea Japan Inc (Tokyo, Japan).

Cell lines and cell culture

KUSA-A1 cells, that was derived from a C3H/He mouse, were maintained in the M061101 medium (okada@med-shirotori.co.jp, MED SHIROTORI Co., Ltd., Tokyo) on 100 mm culture dishes (Falcon 3003; Becton Dickinson Labware, Bedford, MA) at 37°C under a humidified atmosphere of 5% CO_2. ST-2 cells were obtained from the RIKEN cell bank, Japan, and were maintained in RPMI 1640 (Invitrogen Corporation, Auckland, New Zealand) supplemented with 10% FCS and 10^{-5}M of 2-ME (GIBCO BRL) at 37°C under a humidified atmosphere of 5% CO_2 in air.

Cell transplantation

Freshly scraped confluent cells (5×10^6) were subcutaneously implanted into BALB/c nu/nu mice (Clea). These animals were sacrificed by cervical dislocation between 3 and 10 weeks after implantation.

Antibodies

Phycoerythrin (PE)-conjugated antibodies to CD4, CD8, CD3, B220, Mac-1, Gr-1, and Tre119 (Pharmingen, San Diego, CA), fluorescein isothiocyanate (FITC)-conjugated antibody to CD34, H-2k (Pharmingen), allophycocy antim (APC)-conjugated antibody to c-kit (Pharmingen), Sca-1 biotinate antibody (Pharmingen), and antibody to CD16/32 (Fc III/II receptor; 1: 100; Fcblock; Pharmingen) were used for flow cytometric analysis.

Flow cytometric analysis

The monoclonal antibodies (mAbs) were either biotinylated or fluoresceinated. Biotinylated mAbs were detected with streptavidin-conjugated Red 613 (Invitrogen Corporation). Cells were incubated for 30 min on ice with CD16/32 (Fc III/II receptor; 1: 100; Fcblock) before staining with the first antibody. Cells were stained with the first antibody, incubated for 30 min on ice, and then washed twice with washing buffer. The secondary antibody was added, and after incubating the cells for 30 min on ice, they were washed twice with washing buffer and suspended in washing buffer. KUSA-A1 cell suspensions were prepared from monolayer cultures by exposure to trypsin (0.02% for 3 min at 37°C), followed by two washes in cold PBS plus 2% FCS and 0.01% sodium azide. After staining with a series of monoclonal antibodies according to manufacturer's protocol, cells were analyzed by fluorescence-activated cell sorter (FACS) with the FACS vantage system (Becton Dickinson, San Jose, CA).

Colony-forming unit in spleen (CFU-S) assay of hematopoietic cells obtained from ectopic bone

Freshly scraped confluent KUSA-A1 cells (5×10^6) were subcutaneously implanted into BALB/c nu/nu mice (Clea). Hematopoietic cells were obtained from ectopic bone marrow generated by KUSA-A1 cells, and were assayed for CFU-S. Bone marrow cells (5×10^5) were implanted into lethally irradiated BALB/c mice, and the number of colonies (Day 12 CFU-S) was counted 12 days after transplantation. Day 12 CFU-S including erythrocytic, granulocytic, megakaryocytic, and lymphocytic lineages are derived from multipotent HSCs and are more potent in terms of repopulating ability than day 8 CFU-S.

Soft X ray system

BALB nu/nu mice were examined by whole body soft X-ray radiography at 25.0 kV and 3.0 mA for 10 sec (SRO-iM50, Sofron, Tokyo) with X-ray RX film (Fuji Photofilm GmbH, Düsseldorf, Germany).

RESULTS

Induction of hematopoiesis by KUSA-A1 cells

When KUSA-A1 cells were implanted into the subcutaneous tissue, solid hard masses (Fig. 1A) were detected 5 weeks later as electron-dense nodules by soft X-ray analysis (Fig. 1B) at all implantation sites, that is, in the dermal tissue right beneath the cutaneous muscle. Histological examination revealed that the implanted cells survived, and some of them showed mitotic figures (Fig. 1C(a)). At 2 weeks following implantation, an osteogenic matrix was formed in the interstitium, but its matrix formation was still scanty (Fig. 1C(b)). And marked formation of capillary vessels containing erythrocytes in their lumen was observed. At 3 weeks, dense immature bone trabeculae with prominent vascular formation and osteoclast induction were seen (Fig. 1C(c)). By 4 weeks, mature bone trabeculae and sinusoids formed (Fig. 1C(d)), and there were mature granulocytic cells in the marrow space. Hematopoiesis began by 3–5 weeks after implantation.

To determine whether the size of the bone generated by KUSA-A1 cells depends on the implanted cell number, we implanted different numbers of KUSA-A1 cells into subcutaneous tissue (Fig. 1D). The results showed that bone size was clearly depending on the number of cells implanted. Nevertheless, hematopoiesis occurred regardless of the number of cells implanted and bone size.

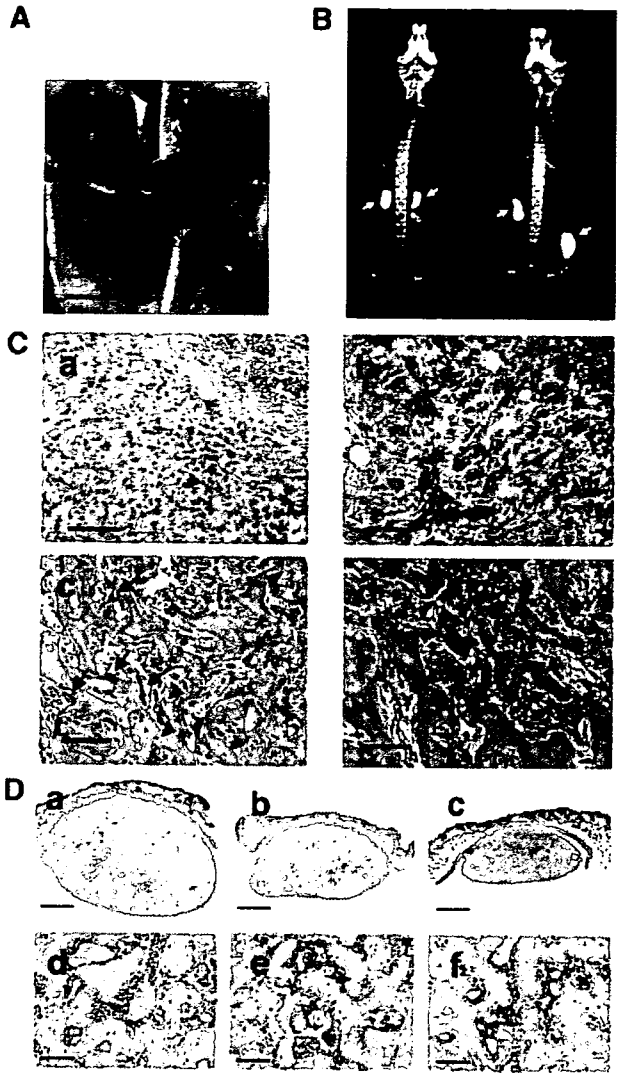

Fig. 1. Time course analysis of hematopoietic induction by KUSA-A1-induced membranous osteogenesis. KUSA-A1 cells were implanted into the subcutaneous tissue of BALB/c nu/nu mice at a density of 2×10^7 cells/200 μl. **A**: Macroscopic view of bone formation at 5 weeks after KUSA-A1 cell injection. **B**: Soft X-ray image of a bone nodule formed by KUSA-A1 cells 5 weeks after implantation. **C**: Histopathological examination of induction of hematopoiesis and bone formation at 1 (**a**), 2 (**b**), 3 (**c**), and 4 (**d**) weeks after KUSA-A1 cell implantation. The mitotic figure of the implanted cell is indicated by an arrowhead (a). Note that numerous osteoclasts (c, arrows) as well as osteoblasts and osteocytes (c, arrowheads) were detected at 3 weeks after implantation. Mature osteocytes were observed at 4 weeks (d, arrowheads). Hematoxylin and eosin stain. Scale bars: 10 mm (A), 230 μm (**C–F**). **D**: Correlation between the number of cells implanted and the size of the bone nodules. Microscopic view of the KUSA-A1 bone 5 weeks after implantation of 2×10^7 (a, d), 1×10^7 (b, e), or 5×10^6 (c, f) KUSA-A1 cells into subcutaneous tissue. Hematoxylin and eosin stain. Scale bars: 2 mm (a–c), 250 μm (d), 300 μm (e), 250 μm (f).

Expression of major histocompatibility antigen (MHC) after implantation

Marrow stromal cells have been reported to be immunologically tolerant, probably due to lack of transplantation antigen expression. To determine whether KUSA-A1 cells are tolerant when implanted into an allogeneic host, KUSA-A1 cells, which are C3H/He mouse origin, were implanted into BALB/c mice (Fig. 2). Time-course analysis clearly revealed that all of the cells were rejected and formed no bone, but numerous foreign body giant cells were observed (Fig. 2C,D), suggesting that KUSA-A1 cells are immunogenic in our experimental setting.

To determine alterations in MHC antigens after implantation, flow cytometric analysis was performed on KUSA-A1 cells (Fig. 2E, open peaks) and cultured mesenchymal cells obtained from KUSA-A1-induced ectopic bone (Fig. 2E, closed peaks) in BALB/c nu/nu mice. The KUSA-A1 cells started to express one of the MHC antigens, H-2k, after implantation into BALB/c nu/nu mice, but expression of Sca-1 was downregulated. Expression of Lin (CD3, CD4, CD8, B220, Gr-1, Mac-1, and Ter119), c-kit, and CD34 remained unchanged after implantation.

MHC expression of the hematopoietic cells in the KUSA-A1 cell-induced bone

Morphological analysis showed that hematopoiesis took place in the KUSA-A1-induced ectopic bone (Fig. 3A–E). Megakaryocytes (arrows in Fig. 3D), erythrocytes (Fig. 3D,E), and granulocytes (Fig. 3D,E) were detected as well as osteoblasts (arrows in Fig. 3E) and mature osteocytes (arrowheads in Fig. 4E). The hematopoietic cells isolated from the KUSA-A1 cell-induced ectopic bone expressed the H-2d antigen, implying that they were derived from the host cells and had not differentiated from the implanted KUSA-A1 cells.

Cytokine production by the implanted KUSA-A1 cells may not be attributable to the migration of hematopoietic cells

To determine whether cytokines, that is, interleukin-6, macrophage-colony stimulating factor, stem cell factor, fms-like tyrosine kinase-3 ligand, and thrombopoietin, were produced by the implanted cells and contributed to the hematopoiesis, ELISA analysis was performed on the serum from mice with cell implantation as well as conditioned medium of the KUSA-A1 cultures (Fig. 3F). RT-PCR analysis of cytokine gene expression revealed that the KUSA-A1 cells express CSF-1, thrombopoietin, angiotensinogen, c-kit ligand, leptin, lymphotoxin A and B, IL4, IL5, IL6, IL10, IL12B, IL16, IL17B, IL19, and angiopoietin1 genes (Supplementary Figure 1S) and transcriptome analysis revealed that KUSA-A1 cells express the SDF-1 gene at a high level (a frequency of 1.1×10^{-3}) (Sharov et al., 2003). However, none of the cytokine levels increased in the serum.

Analysis of KSL cells in the femur and the ectopic bone, and CFU-S in the peripheral blood and the ectopic bone

To investigate whether HSCs as well as mature hematopoietic cells migrates into the ectopic bone, the proportion of KSL cells was examined. The proportion was found to be the same, that is, 0.08%, in both the host femur (Fig. 4A) and the KUSA-A1 ectopic bone (Fig. 4B), suggesting that the ectopic bone as well as native bone serves microenvironment for HSCs.

The number of CFU-S were also counted in the host femur, peripheral blood, and KUSA-A1-induced bone marrow (Fig. 4C–E), and were found to account for $11.2 \pm 0.8/1.0 \times 10^5$ the cells in the KUSA-A1-induced ectopic bone (Fig. 4E, right). By day 12 the CFU-S of the host femur had increased from 28.3 ± 6.0 to $35.0 \pm 3.4/10^5$ cells (Fig. 4E, left). At day 12 CFU-S were also detected in the peripheral blood from the mice and

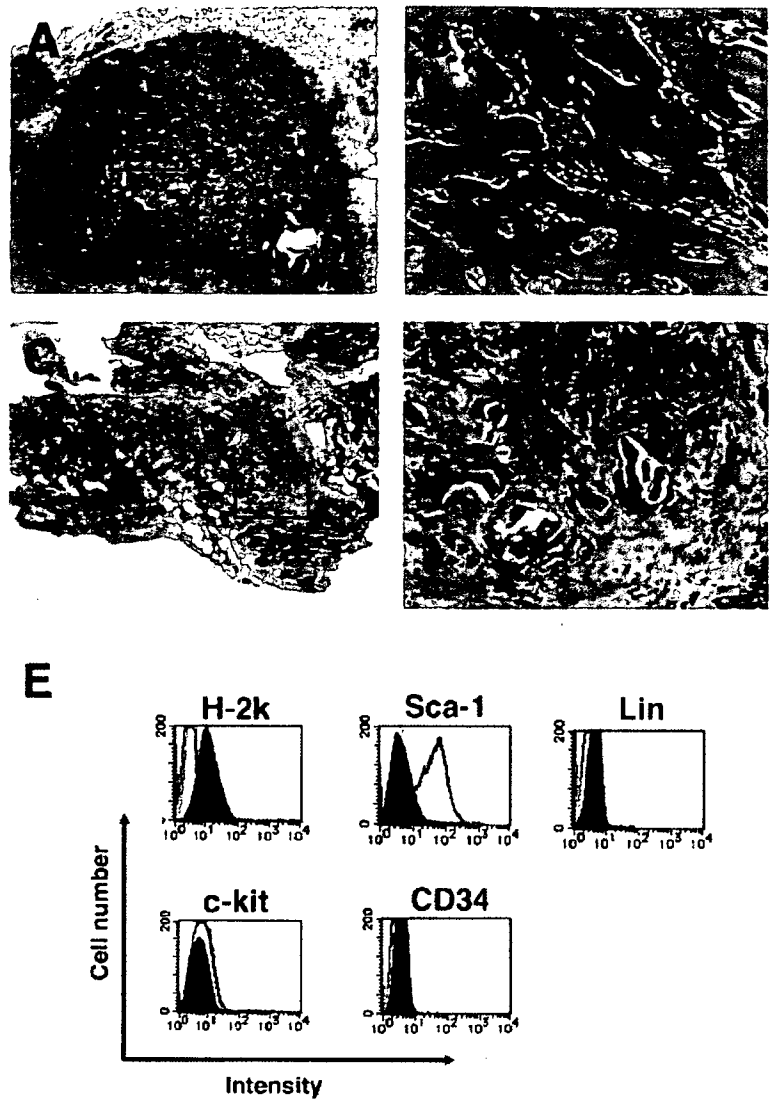

Fig. 2. Rejection of the implanted KUSA-A1 cells in an allogeneic combination. Microscopic view of the generated bone 18 days after the implantation of 5×10^6 KUSA-A1 cells, which were derived from C3H/He mice, into the subcutaneous tissue of syngeneic C3H/He mice (**A, B**) or allogeneic BALB/c mice (**C, D**). Hematoxylin and eosin stain. Parts B and D are higher magnifications of A and C, respectively. **E**: Alterations in cell surface antigens after implantation. Flow cytometric analysis was performed on KUSA-A1 cells (open peaks) and cultured mesenchymal cells obtained from KUSA-A1 ectopic bone (closed peaks) in BALB/c nu/nu mice. The mesenchymal cells were obtained from the KUSA-A1 ectopic bone, and analyzed by flow cytometry. One of major histocompatibility antigens, H-2k, was upregulated, and Sca-1 antigen was downregulated.

accounted for $7.0 \pm 1.7/10^6$ cells (Fig. 4E, middle). In contrast, no CFU-S was detected in the peripheral blood from the mice without KUSA-A1 cell implantation.

Since the upregulation of HSCs in the femurs from the KUSA-A1 cell-implanted mice was rather surprising to us, the time-course of the KSL cell numbers in the femurs from the mice with KUSA-A1 ectopic bone was investigated (Fig. 4F). The number of KSL cells started to increase at 3 weeks, continued to increase to 0.47% by 5 weeks, returned to the basal level, that is, 0.08% at 6 weeks, and then fell down to 0.07% at 7 weeks, implying that the HSC number is strongly correlated with the process of dynamic membranous osteogenesis at the implanted site.

DISCUSSION

Bone remodeling occurs continuously throughout life, and HSCs may mobilize during this remodeling process. The finding in this study support such hypothesis that a very specific niche may be functionally enhanced by bone remodeling (Watt and Hogan, 2000), while a stable or static microenvironment does not support hematopoietic mobilization. For example, accelerated bone remodeling by physical exercise and Vitamin D intake trigger increasing mobilization of HSCs. On the other hand, lack of dynamic bone remodeling in bedridden elderly, astronauts, dieters, postmenopausal women, and patients immobilized for long periods results in downregulation of HSCs in bone marrow.

Upregulation of HSCs by "dynamic" membranous ossification of implanted KUSA-A1 osteoblasts

The cell implantation-based strategy employed in this study revealed that increased niche size following subcutaneous implantation of an osteoblast cell line in syngeneic or immunodeficient mice resulted in

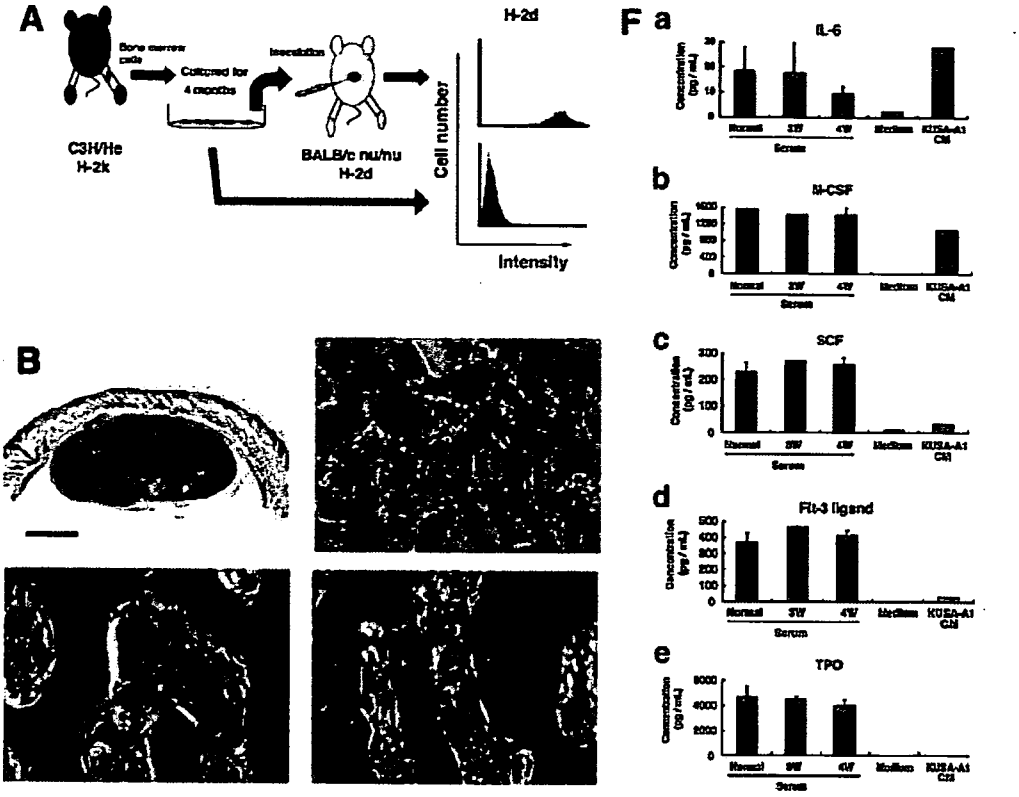

Fig. 3. Hematopoietic cells of host origin in the ectopic bone and serum levels of cytokines after subcutaneous implantation of KUSA-A1 cells. **A**: Flow cytometric analysis of the H-2d antigen in the hematopoietic cells of ectopic bone and KUSA-A1 cells in vitro. The hematopoietic cells in KUSA-A1 bone were examined for expression of the H-2d antigen of the host mice. **B–E**: Histopathological appearance of the hematopoietic cells used for flow cytometric analysis. Trilineage cells, that is, megakaryocytes (D, arrows), erythroblasts (D, E), and granulocytes (E), were observed. Osteoblasts and mature osteocytes are indicated by arrows and arrowheads, respectively (E). Scale bars: 2 mm (B), 400 μm (C), 100 μm (D, E). **F**: Serum levels of interleukin-6 (IL-6) (**a**), macrophage-colony stimulating factor (M-CSF) (**b**), stem cell factor (SCF) (**c**), fms-like tyrosine kinase-3 (Flt-3) ligand (**d**), and thrombopoietin (TPO) (**e**), measured by the ELISA method. The blood samples were obtained at 5 weeks after implantation.

increases in the HSC population. In the HSC population, both the CFU-S and KSL cells increased. The niche that regulates the generation and differentiation of the HSCs was formed following KUSA-A1 cell implantation, and subsequent membranous ossification in vivo. The enlarged area of niche, that is, the inner surface of bone during the dynamic process of membranous osteogenesis may account for the dramatic upregulation of HSCs in the host bone marrow. Once the osteogenic process is terminated, the number of osteoclasts decreases and no bone is remodeled. Furthermore, the number of the KSL cells returns to the basal level in host bone marrow. These facts suggest a correlation between the osteogenic process (Fig. 1C) and increasing number of KSL cells (Fig. 4F).

The source of the CFU-S in the peripheral blood of the mice implanted with KUSA-A1 osteoblasts may be the bone marrow of (a) the ectopic bone; (b) the host femur; (c) both the ectopic bone and the host femur (Fig. 4C). Mobilization of CFU-S from ectopic bone into the peripheral blood is the most likely cause since the induction of HSCs was accompanied by dynamic osteogenesis. The increased HSC number in the host bone marrow can be explained by HSC mobilization from ectopic bone into the peripheral blood. In the normal mice, such migration or mobilization of hematopoietic cells occurs during development. Hematopoietic events in the mouse begin in the yolk sac and aorta-gonad-mesonephros region at day 7 of gestation, and they shift the site to the fetal liver at mid-gestation followed by the bone marrow shortly before birth. The prevailing notion has been that this sequence reflects the migration of HSCs from the yolk sac to the definitive hematopoietic sites. Observation in this study, that is, the generation of ectopic bone in the subcutaneous tissues and the resultant migration of HSCs via the peripheral blood, seems to mimic above process during developments (Dzierzak et al., 1998).

Unexpected upregulation of MHC antigen after implantation of donor cells

Although most HSCs have been reported to express MHCs, that is, HLA in humans, and H-2 antigens in mice, no mesenchymal stem cells have been reported to express MHC antigens at least in vitro (Jiang et al., 2002). Since lack of these antigens on the cell surface may contribute to the induction of tolerance in these cells when transplanted in allogeneic combination, the complete rejection of the transplanted mesenchymal cells and de novo expression of the H-2 antigen after in vivo implantation was contrary to our expectation. We do not know the molecular mechanisms responsible for upregulated expression of H-2 and downregulated expression of Sca-1 after cell implantation, but care should be exercised when mesenchymal cells are implanted for therapeutic purposes, because membrane-bound molecules, including functionally essential molecules, might be modulated after implantation.

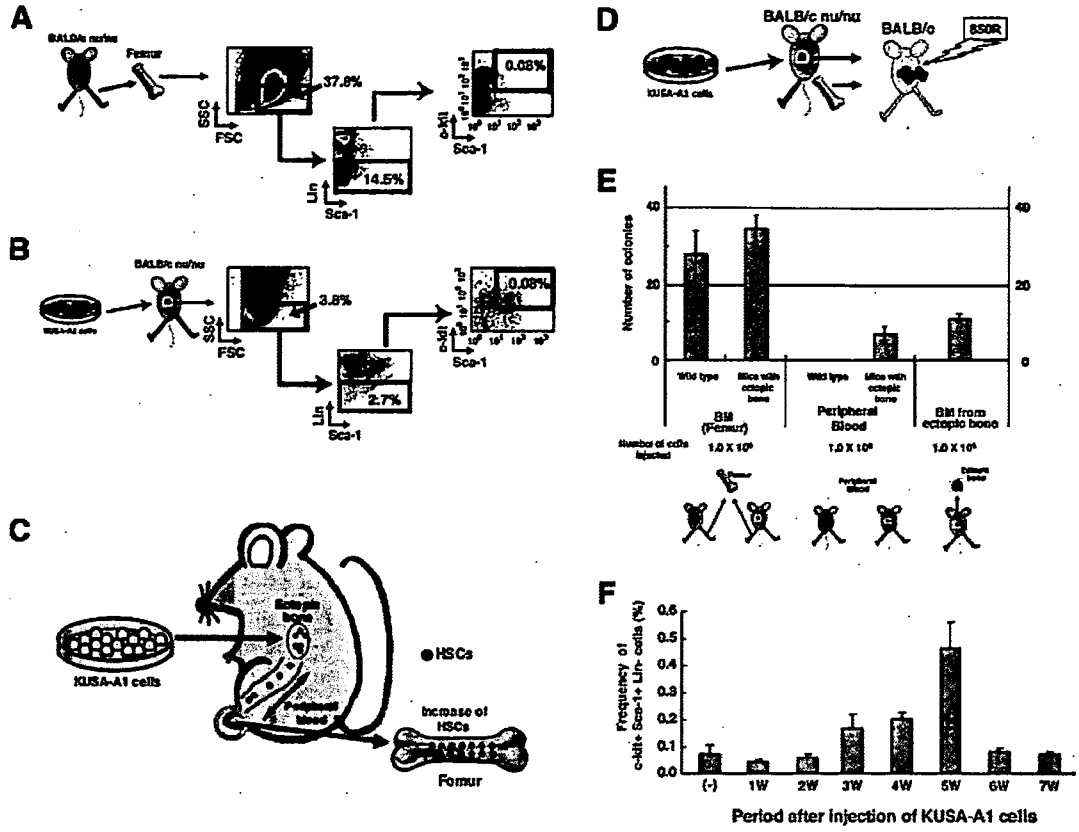

Fig. 4. Mobilization of c-kit$^+$ Sca-1$^+$ Lin$^-$ (KSL) cells in the ectopic bones generated by KUSA-A1 cells. **A** and **B**: Flow cytometric analysis of hematopoietic stem cell markers was performed on hematopoietic cells in the femur of BALB/c nu/nu mice (A) and the ectopic bone generated in BALB/c nu/nu mice (B). KSL cells accounted for 0.08% of the hematopoietic cells in KUSA-A1 bone. **C**: Proposed mechanism of HSC mobilization in the peripheral blood of mice with the ectopic bone, and the increased HSCs in the femur of mice implanted with osteoblasts. Osteoblastic cells whose number has been increased by local injection into the tissues support an increase in number of HSCs in both bone marrow and peripheral blood, as a result of an increase in size of the microenvironment or niche in vivo. The niche size defined by dynamic osteogenic process affects the number of stem cells. **D**: Experimental design to investigate mobilization of CFU-S in the peripheral blood of mice with the ectopic bone, and the proportion of KSL cells in the femur of mice implanted with KUSA-A1 cells. Hematopoiesis was induced in the ectopic bone by KUSA-A1 cell implantation (See Fig. 3). The hematopoietic cells in the ectopic bone and the host femur were analyzed for further CFU-S analysis in mice exposed to 850 cGy irradiation. **E**: CFU-S assay in the marrow cells of the femur of mice not implanted with any cells; the femoral marrow cells of mice with ectopic bone; peripheral blood cells of mice not implanted with cells; peripheral blood cells of mice with ectopic bone; marrow cells in ectopic bone. The blood samples were obtained at 5 weeks after implantation. The number of HSC or CFU-s increased to $11.2 \pm 0.8/1.0 \times 10^6$ cells in the KUSA-A1-induced ectopic bone. CFU-s in the peripheral blood increased to $7.0 \pm 1.7/10^6$ cells at day 12 after implantation of the KUSA-A1 cells while no CFU-s were detected in the peripheral blood from mice without cell implantation. **F**: Time course of the proportion of KLS cells in the femur of mice implanted with KUSA-A1 cells.

Crucial role of marrow stromal subsets in HSC regulation

HSCs are a subset of bone marrow cells that are capable of self-renewal and of forming all types of blood cells. The increases in bone size generated by the spindle-shaped KUSA-A1 osteoblasts correlated with the increase in the number of HSCs. The osteoblasts and a subpopulation of the HSCs expressed N-cadherin, a cell-surface molecule that helps cells adhere to one another, and N-cadherin and -catenin may form important components of the interaction between HSCs and their niche (Zhang et al., 2003). The Notch signaling pathway is also known to regulate cell-fate decisions in many organisms (Calvi et al., 2003). Involvement of cytokine signaling in HSC regulation has been reported to be crucial to the development of blood-forming tissue in embryos. The doubling of bone size mirrored the increase in the HSC population in the mice implanted with KUSA-A1 cells.

The strategy to increase the size of the HSC population by implanting osteoblasts into the subcutaneous tissue to increase the osteoblast cell population may be proven to be of certain clinical value in the future. The concept that a microenvironment or niche controls HSCs may be useful for HSC expansion in vivo, and has potential implications for HSC harvesting and recovery after transplantation (Fig. 4C). Direct implantation of KUSA-A1 cells into syngeneic or immunodeficient mice, in order to better understand the interactions between HSCs and bone marrow, may therefore lead to the development of practical methods of manipulating stem cells and define a model for investigating the impact of the microenvironment on cell physiology (Li et al., 2000). Cellular and molecular identification using the strategy of niche-constituent cells or signaling pathways will provide pharmacological targets with therapeutic potential for stem-cell-based therapies.

ACKNOWLEDGMENTS

This study was supported by a grant from the Ministry of Education, Culture, Sports, Science, and Technology (MEXT) of Japan and the Health and Labour Sciences Research Grants, and the Pharmaceuticals and Medical

Devices Agency to A. U. We thank T. Tsurumi and T. Shimizu for their excellent technical assistance in animal and cell culture.

LITERATURE CITED

Calvi LM, Adams GB, Weibrecht KW, Weber JM, Olson DP, Knight MC, Martin RP, Schipani E, Divieti P, Bringhurst FR, Milner LA, Kronenberg HM, Scadden DT. 2003. Osteoblastic cells regulate the haematopoietic stem cell niche. Nature 425:841–846.

Dzierzak E, Medvinsky A, de Bruijn M. 1998. Qualitative and quantitative aspects of haematopoietic cell development in the mammalian embryo. Immunol Today 19:228–236.

Goodell MA, Brose K, Paradis G, Conner AS, Mulligan RC. 1996. Isolation and functional properties of murine hematopoietic stem cells that are replicating in vivo. J Exp Med 183:1797–1806.

Harrison DE, Russell ES. 1972. The response of W-W v and Sl-Sl d anaemic mice to haemopoietic stimuli. Br J Haematol 22:155–168.

Ikehara S. 2000. Pluripotent hemopoietic stem cells in mice and humans. Proc Soc Exp Biol Med 223:149–155.

Jiang Y, Jahagirdar BN, Reinhardt RL, Schwartz RE, Keene CD, Ortiz-Gonzalez XR, Reyes M, Lenvik T, Lund T, Blackstad M, Du J, Aldrich S, Lisberg A, Low WC, Largaespada DA, Verfaillie CM. 2002. Pluripotency of mesenchymal stem cells derived from adult marrow. Nature 418:41–49.

Kohyama J, Abe H, Shimazaki T, Koizumi A, Nakashima K, Gojo S, Taga T, Okano H, Hata J, Umezawa A. 2001. Brain from bone: Efficient "meta-differentiation" of marrow stroma-derived mature osteoblasts to neurons with Noggin or a demethylating agent. Differentiation 68:235–244.

Li Y, Hisha H, Inaba M, Lian Z, Yu C, Kawamura M, Yamamoto Y, Nishio N, Toki J, Fan H, Ikehara S. 2000. Evidence for migration of donor bone marrow stromal cells into recipient thymus after bone marrow transplantation plus bone grafts: A role of stromal cells in positive selection. Exp Hematol 28:950–960.

Lord BI. 1990. The architecture of bone marrow cell populations. Int J Cell Cloning 8:317–331.

Makino S, Fukuda K, Miyoshi S, Konishi F, Kodama H, Pan J, Sano M, Takahashi T, Hori S, Abe H, Hata J, Umezawa A, Ogawa S. 1999. Cardiomyocytes can be generated from marrow stromal cells in vitro. J Clin Invest 103:697–705.

Matsuzaki Y, Kinjo K, Mulligan RC, Okano H. 2004. Unexpectedly efficient homing capacity of purified murine hematopoietic stem cells. Immunity 20: 87–93.

Mori T, Kiyono T, Imabayashi H, Takeda Y, Tsuchiya K, Miyoshi S, Makino H, Matsumoto K, Saito H, Ogawa S, Sakamoto M, Hata J-I, Umezawa A. 2005. Combination of hTERT and Bmi-1, E6 or E7 induce prolongation of the life span of bone marrow stromal cells from an elderly donor without affecting their neurogenic potential. Mol Cell Biol 25:5183–5195.

Okada S, Nakauchi H, Nagayoshi K, Nishikawa S, Miura Y, Suda T. 1991. Enrichment and characterization of murine hematopoietic stem cells that express c-kit molecule. Blood 78:1706–1712.

Okada S, Nakauchi H, Nagayoshi K, Nishikawa S, Miura Y, Suda T. 1992. In vivo and in vitro stem cell function of c-kit- and Sca-1-positive murine hematopoietic cells. Blood 80:3044–3050.

Osawa M, Hanada K, Hamada H, Nakauchi H. 1996. Long-term lymphohematopoietic reconstitution by a single CD34-low/negative hematopoietic stem cell. Science 273:242–245.

Pittenger MF, Mackay AM, Beck SC, Jaiswal RK, Douglas R, Mosca JD, Moorman MA, Simonetti DW, Craig S, Marshak DR. 1999. Multilineage potential of adult human mesenchymal stem cells. Science 284:143–147.

Schöfield R. 1978. The relationship between the spleen colony-forming cell and the haemopoietic stem cell. Blood Cells 4:7–25.

Sharov AA, Piao Y, Matoba R, Dudekula DB, Qian Y, VanBuren V, Falco G, Martin PR, Stagg CA, Bassey UC, Wang Y, Carter MG, Hamatani T, Aiba K, Akutsu H, Sharova L, Tanaka TS, Kimber WL, Yoshikawa T, Jaradat SA, Pantano S, Nagaraja R, Boheler KR, Taub D, Hodes RJ, Longo DL, Schlessinger D, Keller J, Klotz E, Kelsoe G, Umezawa A, Vescovi AL, Rossant J, Kunath T, Hogan BL, Curci A, D'Urso M, Kelso J, Hide W, Ko MS. 2003. Transcriptome analysis of mouse stem cells and early embryos. PLoS Biol 1:E74.

Siminovitch L, McCulloch EA, Till JE. 1963. The distribution of colony-forming cells among spleen colonies. J Cell Physiol 62:327–336.

Spangrude GJ, Heimfeld S, Weissman IL. 1988. Purification and characterization of mouse hematopoietic stem cells. Science 241:58–62.

Takeda Y, Mori T, Imabayashi H, Kiyono T, Gojo S, Miyoshi S, Hida N, Ita M, Segawa K, Ogawa S, Sakamoto M, Nakamura S, Umezawa A. 2004. Can the life span of human marrow stromal cells be prolonged by bmi-1, E6, E7, and/or telomerase without affecting cardiomyogenic differentiation? J Gene Med 6:833–845.

Terai M, Uyama T, Sugiki T, Li XK, Umezawa A, Kiyono T. 2005. Immortalization of human fetal cells: the life span of umbilical cord blood-derived cells can be prolonged without manipulating p16INK4a/RB braking pathway. Mol Biol Cell 16:1491–1499.

Till JE, McCulloch CE. 1961. A direct measurement of the radiation sensitivity of normal mouse bone marrow cells. Radiat Res 14:213–222.

Till JE, McCulloch EA, Siminovitch L. 1964. A stochastic model of stem cell proliferation, based on the growth of spleen colony-forming cells. Proc Natl Acad Sci USA 51:29–36.

Umezawa A, Maruyama T, Segawa K, Shadduck RK, Waheed A, Hata J. 1992. Multipotent marrow stromal cell line is able to induce hematopoiesis in vivo. J Cell Physiol 151:197–205.

Watt FM, Hogan BL. 2000. Out of Eden: Stem cells and their niches. Science 287:1427–1430.

Weissman IL. 2000. Stem cells: Units of development, units of regeneration, and units in evolution. Cell 100:157–168.

Yoshimoto M, Shinohara T, Heike T, Shiota M, Kanatsu-Shinohara M, Nakahata T. 2003. Direct visualization of transplanted hematopoietic cell reconstitution in intact mouse organs indicates the presence of a niche. Exp Hematol 31: 733–740.

Zhang J, Niu C, Ye L, Huang H, He X, Tong WG, Ross J, Haug J, Johnson T, Feng JQ, Harris S, Wiedemann LM, Mishina Y, Li L. 2003. Identification of the haematopoietic stem cell niche and control of the niche size. Nature 425: 836–841.

0013-7227/06/$15.00/0
Printed in U.S.A.

Endocrinology 147(9):4104–4111

doi: 10.1210/en.2006-0162

Differentiation of Adult Stem Cells Derived from Bone Marrow Stroma into Leydig or Adrenocortical Cells

Takashi Yazawa, Tetsuya Mizutani, Kazuya Yamada, Hiroko Kawata, Toshio Sekiguchi, Miki Yoshino, Takashi Kajitani, Zhangfei Shou, Akihiro Umezawa, and Kaoru Miyamoto

Department of Biochemistry (T.Y., T.M., K.Y., H.K., T.S., M.Y., T.K., Z.S., K.M.), Faculty of Medical Sciences, University of Fukui, Fukui 910-1193, Japan; Core Research for Evolutional Science and Technology (T.Y., T.M., K.Y., H.K., T.S., M.Y., T.K., Z.S., K.M.), Japan Science and Technology Agency, Saitama 332-0012, Japan; and National Research Institute for Child Health and Development (A.U.), Tokyo 157-8535, Japan

Adult stem cells from bone marrow, referred to as mesenchymal stem cells or marrow stromal cells (MSCs), are defined as pluripotent cells and have the ability to differentiate into multiple mesodermal cells. In this study, we investigated whether MSCs from rat, mouse, and human are able to differentiate into steroidogenic cells. When transplanted into immature rat testes, adherent marrow-derived cells (including MSCs) were found to be engrafted and differentiate into steroidogenic cells that were indistinguishable from Leydig cells. Isolated murine MSCs transfected with green fluorescence protein driven by the promoter of P450 side-chain cleaving enzyme gene (CYP11A), a steroidogenic cell-specific gene, were used to detect steroidogenic cell production *in vitro*. During *in vitro* differentiation, green fluorescence protein-positive cells, which had characteristics similar to those of Leydig cells, were found. Stable transfection of murine MSCs with a transcription factor, steroidogenic factor-1, followed by treatment with cAMP almost recapitulated the properties of Leydig cells, including the production of testosterone. Transfection of human MSCs with steroidogenic factor-1 also led to their conversion to steroidogenic cells, but they appeared to be glucocorticoid- rather than testosterone-producing cells. These results indicate that MSCs represent a useful source of stem cells for producing steroidogenic cells that may provide basis for their use in cell and gene therapy. (*Endocrinology* 147: 4104–4111, 2006)

STEM CELLS ARE self-renewing elements with the capacity to generate multiple distinct cell lineages. They exist in various tissues, even in adults, and have been isolated from a variety of differentiated tissues, including bone marrow, umbilical blood, brain, and fat (1–6). Among these, bone marrow-derived mesenchymal stem cells (MSCs), also known as marrow stromal cells, are defined as pluripotent cells and have been shown to differentiate into adipocytes, chondrocytes, osteoblasts, and hematopoietic-supporting stroma both *in vivo* and *ex vivo* (1–3). Furthermore, they are able to generate cells of all three germ layers (7, 8). In addition to their multipotency for differentiation, MSCs have attracted considerable interest for use in cell and gene therapy because these cells can easily be obtained from adult marrow tissue (8–10).

The gonad and adrenal gland are the primary steroidogenic organs in mammals. In the gonad, male Leydig cells or female granulosa and theca cells are responsible for the production of androgens and estrogens. The adrenal cortex produces glucocorticoids and mineralocorticoids, although some androgens are also produced in many species, except rodents. These steroidogenic organs develop from the common adrenogenital primodium, which originates from the intermediate mesoderm (11). Fetal-type steroidogenic cells appear when the adrenogenital primodium differentiates into the adrenal cortex and the gonads of the two sexes. These are replaced by adult-type steroidogenic cells during the period between birth and puberty (12, 13), but these processes are poorly understood.

One approach to resolving the complexities of organogenesis is to use stem cells as a model system for differentiation. In this study, the differentiation of MSCs into steroidogenic cells was examined *in vivo* and *in vitro* by several methods. A number of studies have reported that the injection of MSCs into some tissues leads to the differentiation of the injected cells into tissue-specific cells, probably due to the microenvironment near the injection sites. To determine whether MSCs are able to differentiate into steroidogenic cells, we injected a purified population of rat MSCs into the prepubertal rat testis and examined the fate of these cells by immunohistochemistry. In addition, the spontaneous differentiation of MSCs to specific cells can be monitored by the expression of specific genes in the differentiated cells. One such experimental approach, known as a promoter-sorting method, is to use fluorescence-activated cell sorting (FACS) to select green fluorescence protein (GFP)-positive MSCs in which the expression of GFP is under the control of the promoter of a gene that is expressed in a cell type-specific fashion. In this study, to demonstrate the emergence of steroidogenic cells from isolated MSCs *in vitro*, a GFP expression vector driven by the CYP11A promoter (CYP11A is a

First Published Online May 25, 2006

Abbreviations: ES, Embryonic stem; FACS, fluorescence activated cell sorting; GFP, green fluorescence protein; hMSC, human MSC; 3β-HSD I, 3β-hydroxysteroid dehydrogenase I; 17β-HSD III, 17β-hydroxysteroid dehydrogenase III; mMSC, murine MSC; MSC, mesenchymal stem cell; P450arom, cytochrome P450 aromatase; P450c17, cytochrome P450 17α-hydroxylase; P450c21, cytochrome P450 steroid 21-hydroxylase; P450scc, P450 side-chain cleaving enzyme; SF, steroidogenic factor; StAR, steroidogenic acute regulatory protein.

***Endocrinology* is published monthly by The Endocrine Society (http://www.endo-society.org), the foremost professional society serving the endocrine community.**